https://doi.org/10.5194/hess-2023-92
Preprint. Discussion started: 20 April 2023


Hydrology and Earth System Sciences
Discussions

# Simulating one century (1902-2009) of river discharges, low flow sequences and flood events of an alpine river from large-scale atmospheric information

Caroline Legrand[1], Benoît Hingray[1], Bruno Wilhelm[1,†], and Martin Ménégoz[1]

[1]Univ. Grenoble Alpes, CNRS, INRAE, IRD, Grenoble INP*, IGE, 38000 Grenoble, France
[1]*Institute of Engineering and Management Univ. Grenoble Alpes
[†]deceased, 5 April 2022

**Correspondence:** Caroline Legrand (caroline.legrand@univ-grenoble-alpes.fr)

**Abstract.** We assess the ability of two typical simulation chains to reproduce, over the last century (1902-2009) and from large-scale atmospheric information only, the temporal variations of river discharges, low flow sequences and flood events, observed at different locations of the Upper Rhône River (URR) catchment, an alpine river straddling France and Switzerland $\left(10,900\,\mathrm{km}^2\right)$. The two simulation chains are made up of a downscaling model, either statistical (SCAMP) or dynamical (MAR), and the glacio-hydrological model GSM-SOCONT. Both downscaling models, forced by atmospheric information from the ERA-20C atmospheric reanalysis, provide time series of daily scenarios of precipitation and temperature used as input to the hydrological model. With hydrological regimes ranging from highly glaciated ones in its upper part to mixed ones dominated by snow and rain downstream, the URR catchment is ideal to evaluate the different simulation chains in contrasting and demanding hydro-meteorological configurations where the interplay between weather variables, both in space and time, is determinant. Whatever the river sub-basin considered, the simulated discharges are in good agreement with the reference ones, provided that the weather scenarios are bias-corrected. The observed multi-scale variations of discharges (daily, seasonal and interannual) are well reproduced and the hydrological situations of low frequency (low flow sequences and flood events) are reasonably well reproduced. Bias correction is crucial for both precipitation and temperature and both downscaling models. For the dynamical one, a bias correction is also essential to get realistic daily temperature lapse rates. Uncorrected scenarios lead to irrelevant hydrological simulations, especially for the sub-catchments at high elevation, mainly due to irrelevant snowpack dynamic simulations. The simulations also highlight the difficulty to simulate precipitation dependency to elevation over mountainous areas.

## 1 Introduction

Climate change is expected to exacerbate flood hazard through an intensification of the hydrological cycle, which will likely alter the magnitude, frequency, and/or seasonality of floods (Blöschl et al., 2017). Another concern is that of future low flows and drought situations, which are also expected to be more frequent, longer and more intense (Ruosteenoja et al., 2018; Masson-Delmotte et al., 2021). However, projecting the possible evolution of hydrological extremes at the catchment scale is

https://doi.org/10.5194/hess-2023-92
Preprint. Discussion started: 20 April 2023


Hydrology and Earth System Sciences
Discussions

still challenging, and although a large number of works has been developed for a number of rivers worldwide, considerable uncertainty about possible future changes remains, both for changes in the intensity and frequency of extreme events (e.g. Kundzewicz et al., 2016; Roudier et al., 2016; Vidal et al., 2016; Di Sante et al., 2021; Evin et al., 2021; Lemaitre-Basset et al., 2021).

Hydrological scenarios required for climate change impact studies are actually commonly obtained by simulation with hydrological models from ensembles of projected meteorological scenarios. To allow for a relevant impact assessment, meteorological scenarios have to fulfill some constraints imposed by the strong non-linearity and the high spatial and temporal variability of hydrological processes (e.g. strong dependence of temperature, radiative fluxes, precipitation, etc, on elevation and aspect in mountainous environments). For instance, the meteorological scenarios have to be bias-corrected (e.g. with respect to space and seasonality) and to have rather high spatial and temporal resolution (Lafaysse et al., 2014). Because such requirements are not fulfilled by General Circulation Models (GCMs), meteorological scenarios are classically obtained with downscaling models, either dynamical or statistical.

Dynamical Downscaling Models (DDMs) are Regional Climate Models (RCMs) nested within the GCM to generate fine resolution climate information (Giorgi and Mearns, 1991). They solve the full equations of mass, energy, and momentum conservation laws in the atmosphere to account for the physical interactions of land-atmosphere processes with consideration of the heterogeneity of topography, soil, vegetation, and climate variables in a region or a catchment. Over the past three decades, RCMs have been widely used in a number of studies for hydrological purposes (e.g. Hay et al., 2002; Arnell et al., 2003; Jha et al., 2004; Leander et al., 2008; Leung and Qian, 2009; Salathé et al., 2014; see Tapiador et al., 2020 for a complete review).

On the other hand, Statistical Downscaling Models (SDMs) are based on empirical relationships identified from observations between large-scale atmospheric variables (or predictors) and local weather variables (or predictands) (Von Storch et al., 1993). Weather scenarios derived from SDMs are produced from time series of predictors extracted from large-scale atmospheric outputs of climate models. SDMs have been widely used to i) generate local weather scenarios for past or future climates from GCM experiments (e.g. Wilby et al., 1999; Hanssen-Bauer et al., 2005; Boé et al., 2007; Lafaysse et al., 2014; Dayon et al., 2015), ii) produce local weather forecasts from large-scale weather forecasts of numerical weather prediction models (e.g. Obled et al., 2002; Gangopadhyay et al., 2005; Marty et al., 2012; Ben Daoud et al., 2016), and iii) produce reconstructions of past weather conditions from atmospheric reanalysis data (e.g. Wilby and Quinn, 2013; Kuentz et al., 2015; Caillouet et al., 2016).

A general discussion of the pros-and-cons of selecting one downscaling approach over the other has been the subject of multiple manuscripts (see Fowler et al., 2007 or Maraun et al., 2010 for a review). DDMs have the advantage of being formulated on physical principles, but their simulations are computationally intensive and time consuming with a resolution that is generally still to coarse to catch local processes. Their are obviously not free of limitations and their outputs often need to be corrected for impact studies. In contrast, SDMs are very popular because of their computational efficiency and ease of use. However, they may sometimes miss some important interactions and/or correlations between meteorological variables, both in space and time.

https://doi.org/10.5194/hess-2023-92
Preprint. Discussion started: 20 April 2023


Hydrology and Earth System Sciences
Discussions

A prerequisite for climate impact analyses is that the modeling chain considered for the simulations is able to reproduce in a relevant way the multi-scale hydrological variations that result from the large-scale atmospheric trajectories of the considered period.

In this work, we assess and compare the ability of two typical simulations chains to reproduce, over the last century (1902-2009) and from large-scale atmospheric information only, the observed temporal variations of discharges, especially those of low flows and flood events, in the Upper Rhône River (URR) catchment. We additionally assess the necessity and the added value of a bias correction step in the elaboration of weather scenarios. The two modeling chains are made up of i) the atmospheric reanalysis ERA-20C (Poli et al., 2016), ii) either the statistical downscaling model SCAMP (Raynaud et al., 2020) or the dynamical downscaling model MAR (Gallée and Schayes, 1994), and iii) the glacio-hydrological model GSM-SOCONT (Schaefli et al., 2005).

The URR catchment is a mesoscale alpine catchment straddling Switzerland and France. With a number of different hydrological regimes, ranging from highly glaciated ones in its upper part to mixed ones dominated by snow and rain downstream, the URR catchment offers a great opportunity to evaluate the different downscaling approaches in contrasting and demanding hydro-meteorological configurations where the interplay between weather variables, both in space and time, is determinant.

The paper is structured as follows. Section 2 describes the study area and Sect. 3 the data. Section 4 presents the components of the different simulation chains. A meteorological and hydrological assessment is carried out in Sect.5. Results are discussed in Sect. 6. Finally, Sect. 7 sums up the main outputs of this study and outlines future research lines.

## 2 Study area

The Upper Rhône River catchment $\left(10,900\,\mathrm{km}^2\right)$ covers the southwestern part of the Swiss Alps and a part of the northern French Alps (Fig. 1). The altitude of this catchment ranges from 300 $\mathrm{m}$ to above 4,800 $\mathrm{m}$ at the top of the Mont Blanc. The presence of steep slopes make this area particularly prone to natural hazards such as landslides, floods and avalanches, which are strongly connected to meteorological conditions (Beniston, 2006; Raymond et al., 2019).

In this region, the climate is continental and the temporal variability of precipitation and temperature is high. Mean annual precipitation ranges from 600 $\mathrm{mm}$ (in some parts of Wallis canton, Switzerland) to 1100 $\mathrm{mm}$ (Chamonix, France). It rains from 30 % to 45 % of the days, with an annual maximum daily precipitation reaching locally 45 $\mathrm{mm\ day}^{-1}$ to 105 $\mathrm{mm\ day}^{-1}$ on average (Isotta et al., 2014). Glaciated areas covered 17 % of the catchment upstream to Lake Geneva and 10 % of the whole catchment in 2019 (GLIMS, 2019).

The gauging station of Bognes (Rhône@Bognes hereafter) records daily mean discharges at the outlet of the URR catchment. It is located at Injoux-Génissiat (France), 46 $\mathrm{km}$ downstream of the confluence of the Rhône and the Arve Rivers. Before the confluence of the two rivers, the hydrological regime of the URR catchment is glacio-nival: the important seasonal snowpack dynamics combined with the late summer contribution of glacier melt result in a strong seasonality of flow. Flood events are observed in spring due to snowmelt and in late summer/fall as a results of events with large to very large rainfall amounts (e.g. the so-called "Binn-Simplon" situations). The URR hydrological regimes turns to pluvio-nival downstream, with the successive

https://doi.org/10.5194/hess-2023-92
Preprint. Discussion started: 20 April 2023




Hydrology and Earth System Sciences
Discussions

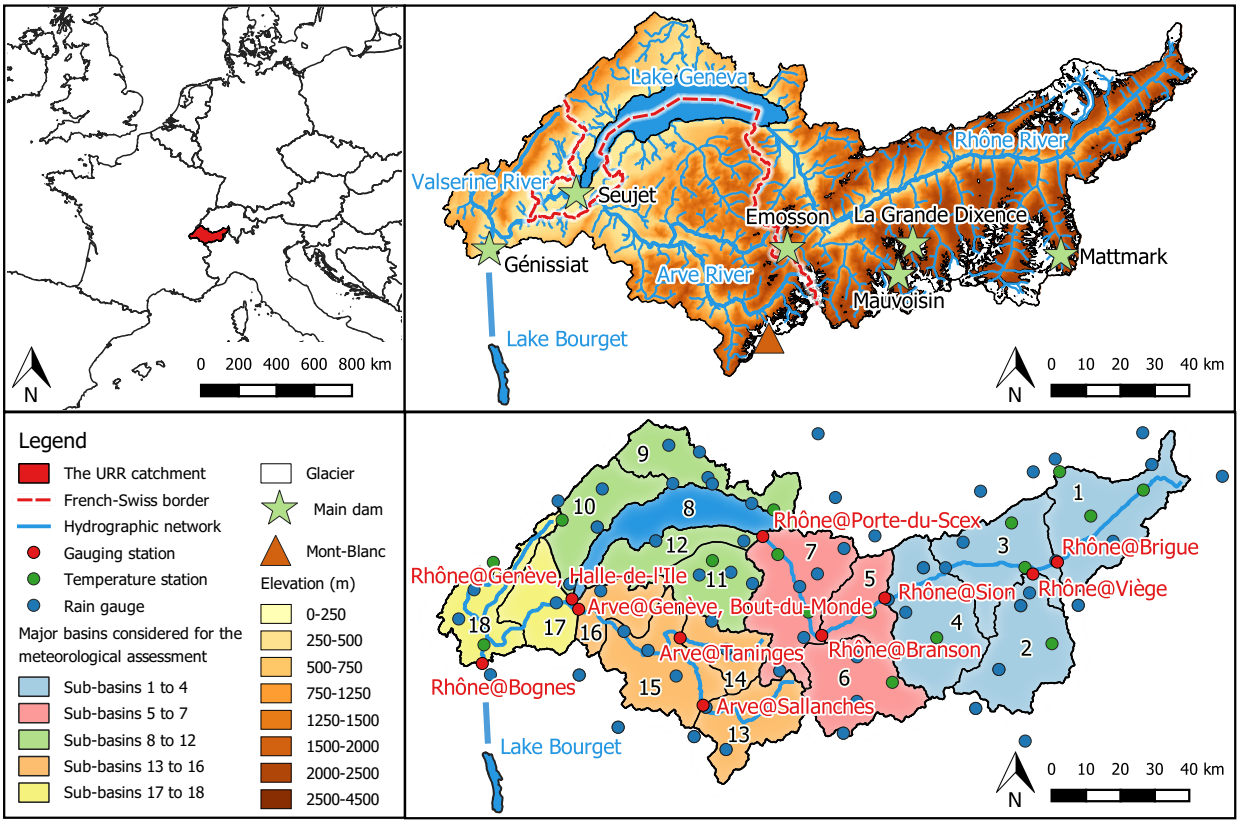


**Figure 1.** Study area. (**top**) Localisation and hydrological characteristics of the URR catchment. (**bottom**) Locations of the different weather and gauging stations.

contributions of lower elevation areas, especially that of the Arve River. Flood events from the Arve River mainly result from extreme rainfall events in fall (e.g. the so-called "retour d'Est events").

Upstream to Lake Geneva, the URR hydrological regime is considered to be natural until the 1950s, before the construction of several large seasonal water reservoirs, mainly used for hydroelectricity production and flood protection. The reservoirs typically store the snow and glacier melt inflows from high elevation areas in spring and summer for hydroelectricity production in winter. The total storage capacity of all reservoirs in the catchment is $1200 \times 10^6$ $\mathrm{m}^3$ or roughly 20 % of the annual catchment precipitation. Since the 1950s, the URR hydrological regime is thus significantly altered, with a reduced seasonality (higher river discharges in winter, smaller ones in spring/summer) and reduced flood discharges in summer and fall (Hingray et al., 2014). Downstream, Lake Geneva, which is the largest natural water reservoir in Western Europe (580 $\mathrm{km}^2$), has a significant natural buffer effect on river flows. Its influence on flows was even exacerbated since 1884 with the construction of a downstream regulation weir for flood protection and hydroelectricity production (Grandjean, 1990).

https://doi.org/10.5194/hess-2023-92
Preprint. Discussion started: 20 April 2023


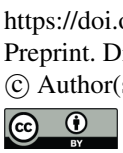

Hydrology and Earth System Sciences
Discussions

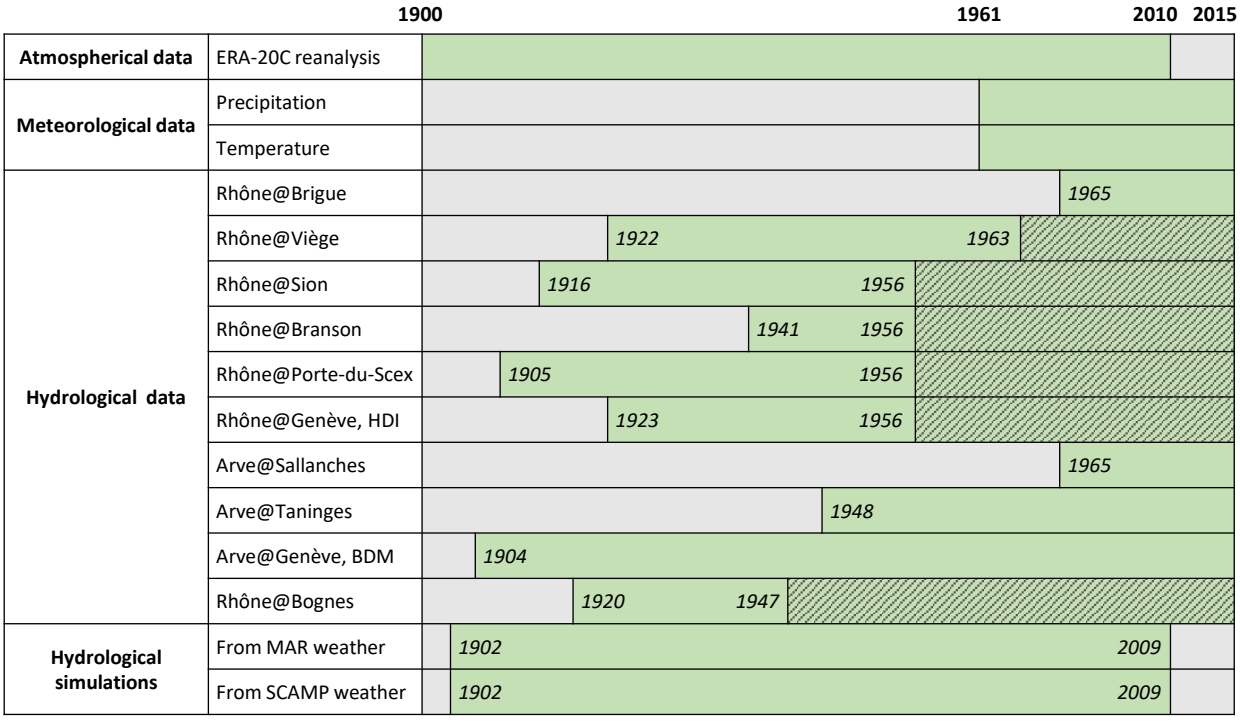


**Figure 2.** Data used. Periods for which daily variables are available are shown in green. Hatchings indicate periods for which the hydrological regime of the URR catchment is significantly altered by dams.

## 3 Data

### 3.1 Meteorological and hydrological data

The density of weather stations covering the URR catchment is rather high. Daily meteorological variables are available from January 1, 1961 to December 31, 2015 for 62 rain gauges and 39 temperature stations in the catchment and in the areas bordering it. The period for which observed daily discharges are available depends on the gauging station. It covers up to one century for the URR at Porte-du-Scex, the outlet of the river to Lake Geneva (Fig. 2). Note that for some basins, there is no observed meteorological data concomitant with "natural" discharge data. Weather and hydrological data were provided by i) the Office Fédéral de l'EnVironnement (OFEV) for the Swiss part, and ii) Météo France and the Banque Hydro for the French part. The observed level of Lake Geneva is also available from OFEV since 1886 at daily time step.

https://doi.org/10.5194/hess-2023-92
Preprint. Discussion started: 20 April 2023


Hydrology and Earth System Sciences
Discussions

### 3.2 Atmospheric data

The ERA-20C reanalysis from the European Centre for Medium-Range Weather Forecasts (ECMWF; Poli et al., 2016) is used i) as boundary conditions for the RCM MAR experiments, and ii) directly as input for the statistical downscaling model SCAMP. This reanalysis provides 6-hourly data over 1900-2010 at a $1.25°$ spatial resolution.

## 4 Methods

### 4.1 Hydrological model

#### 4.1.1 The GSM-SOCONT model

The discharge simulations have been performed with a semi-distributed and daily configuration of GSM-SOCONT (Glacier and SnowMelt SOil CONTribution model; Schaefli et al., 2005), a bucket-type model that uses time series of Mean Areal Precipitation (MAP) and Temperature (MAT) as inputs for each hydrological unit. The URR catchment is distributed over 18 sub-basins, following Obled et al. (2009) with an additional criteria considering the availability of discharge observations. The ice-covered and the ice-free parts of each sub-basin, extracted from the Global Land Ice Measurements from Space (GLIMS, 2019), are considered separately and divided into 500 $\mathrm{m}$ elevation bands. For each elevation band, further referred to as Relatively Homogeneous Hydrological Unit (RHHU), a daily potential evapotranspiration time series is derived from temperature. The regional temperature-evapotranspiration relationship used for this was estimated on a monthly basis from the CRU (Climate Research Unit) potential evapotranspiration and temperature estimates produced for the 1900-2010 period (Harris et al., 2014).

For each RHHU, daily MAP and MAT are estimated from neighboring weather stations using the Thiessen's weighting method and a regional and time varying elevation-temperature relationship (Hingray et al., 2010). MAT is estimated for the mean RHHU elevation. MAP is supposed to be solid if MAT is smaller than a critical temperature $\mathrm{Tc}_1$, liquid if MAT is higher than a critical temperature $\mathrm{Tc}_2$, and mixed otherwise. The $\mathrm{Tc}_1$ and $\mathrm{Tc}_2$ values are fixed to $0\ °\mathrm{C}$ and $2\ °\mathrm{C}$ following Froidurot et al. (2014).

For each RHHU, the snowpack temporal evolution is computed based on MAP and MAT time series. Each simulation day, solid and/or liquid precipitation are added to the snowpack storage and/or to its liquid water content respectively. The liquid water content is also increased by snowmelt if any and the snowpack is increased by refreezing water if any. Snowmelt (or refreezing water) is estimated with a degree-day model from the positive (respectively negative) temperature degrees of the day. When the liquid water content reaches the snowpack retention capacity, an "equivalent rainfall" is released. The retention capacity is assumed to be proportional to the snowpack water equivalent following Kuchment and Gelfan (1996). For glaciated RHHUs, ice melt can additionally occur, namely when the glacier surface is free of snow. Ice melt is also estimated with a degree-day model.

https://doi.org/10.5194/hess-2023-92
Preprint. Discussion started: 20 April 2023


Hydrology and Earth System Sciences
Discussions

For glaciated RHHUs, the rainfall and meltwater-runoff transformation is completed through two linear reservoirs, one for ice melt and one for the rainfall or equivalent rainfall. For non-glaciated RHHUs, the rainfall or equivalent rainfall is separated into infiltration and effective rainfall. Infiltration feeds a non-linear soil reservoir which produces deep infiltration and sub-surface flow. Infiltration (resp. actual evapotranspiration) is estimated from equivalent rainfall (resp. potential evapotranspiration) and simulated soil moisture. Effective rainfall feeds a linear overland reservoir which produces direct runoff.

The discharge simulated at the outlet of each sub-basin is the sum of the different discharge components produced by the different RHHUs from the glaciated and non-glaciated areas of the sub-basin. Discharges simulated for the 18 sub-basins are routed within the hydrological network producing the discharge at each gauging station and at the catchment outlet.

Seven parameters have to be estimated for each ice-free RHHU (e.g. snowmelt degree-day factor, storage capacity and recession coefficient of reservoirs). Three additional parameters have to be estimated for glaciated RHHUs (ice melt degree-day factor, and recession coefficient of ice and snow reservoirs).

#### 4.1.2 Hydrological model calibration

In most cases (as in here), hydrological models simulate the natural behavior of the considered catchments. One frequent approach for estimating the model parameters in such a configuration requires a time period with concomitant observations of weather and "natural" discharges, i.e. concomitant observations of weather and discharges not altered by anthropic activities or waterworks. For most sub-basins of the URR catchment, there is no such period. Daily weather observations are mainly available from the 1960s (here for period P1 = 1961-2015) whereas their hydrological behavior was natural until the 1950s only, strongly altered after by the dams.

The method used for parameter estimation was thus adapted to the catchment data configuration, depending i) on the "perturbation" level of the catchment hydrological behavior during period P1, and ii) on the availability of flow observation records for the period prior the 1950s. For gauged catchments for which the hydrological behavior can be considered as natural (or at least not significantly altered) over period P1 (or at least over a significant sub-period of P1), parameters were estimated with a classical hydrological calibration approach, minimizing an objective function estimated from simulated and observed discharges time series on the same period, namely:

$$F_{natural} = 1 - NSE_{chrono} \quad (1)$$

where $NSE_{chrono}$ is the Nash-Sutcliffe Efficiency criterion (Nash and Sutcliffe, 1970) obtained from day-to-day deviations between observed and simulated daily discharges.

For gauged catchments for which the hydrological behavior is significantly altered over P1 and for which "natural" flow observations are available prior to 1950, parameters were estimated based on hydrological signatures (Sivapalan et al., 2003; Winsemius et al., 2009). In the present case, parameters are calibrated so that simulated signatures reproduce at best observed ones but observed and simulated signatures come from different periods following Hingray et al. (2010) (e.g. 1961-2015 and 1922-1963 respectively for the Viège basin). We thus assume that the weather regimes and the natural hydrological behavior of the catchment have not significantly changed over the last century, which seems a reasonable assumption to make in first

https://doi.org/10.5194/hess-2023-92
Preprint. Discussion started: 20 April 2023


Hydrology and Earth System Sciences
Discussions

approximation. Signatures considered here are the interannual daily regime (366 values) and the statistical distribution of the annual discharge maxima. The objective function is a combination of the NSE criterion and the Kolmogorov-Smirnov distance $d_{KS}$, applied respectively between simulated and observed signatures:

$$F_{altered} = 0,5 * (1 - NSE_{regime}) + 0,5 * \frac{d_{KS}}{\max(Q_{obs_{KS}}, Q_{sim_{KS}})} \quad (2)$$

where $d_{KS} = |Q_{obs_{KS}} - Q_{sim_{KS}}|$ is the Kolmogorov-Smirnov distance with $Q_{obs_{KS}}$ and $Q_{sim_{KS}}$ the corresponding discharge percentiles in the observed and simulated distributions.

The objective functions values obtained for sub-basins calibrated from signatures are given in Supplementary Materials (Table S1). The results of this signature-based calibration are illustrated with the results obtained for the Viège basin in Fig. S2.

Finally, for ungauged basins, parameters were obtained via regionalization from neighboring gauged basins, following the methodological recommendations of Bárdossy (2007) and Viviroli et al. (2009). In practice, whatever the calibration configuration and the calibration objective function, we used the automatic calibration algorithm DDS (Dynamically Dimensioned Search; Tolson and Shoemaker, 2007).

#### 4.1.3 Modeling of the behavior of Lake Geneva

An ad hoc model was developed to simulate the influence of Lake Geneva on river flows. The lake has a natural buffer effect on flows, additionally altered with its regulation. From the 1990s, the outflows first follow the main regulation objectives of the 1997 settlement (CERCG, 1997), namely i) a target water level in the lake for each calendar day, ii) the environmental low flow to be satisfied downstream, and iii) the discharge to not exceed except during periods of high water in the lake. The day-to-day variations of lake outflows are additionally driven by the hydroelectric production required from the plant at the lake outlet to satisfy a part of the regional electricity demand.

By lack of appropriate data, we here only accounted for the natural buffer effect of the lake and for the main regulation objectives mentioned above. The natural buffer effect was simply modeled with the classical three equations system needed to simulate the behavior of unregulated reservoirs, namely a water balance, a storage and a reservoir flow equation (Hingray et al., 2014). Here, a simple linear water level-storage relationship is considered and the outflow that would be obtained without regulation is assumed to be proportional to the volume stored in the reservoir. For the water balance, changes in storage are obtained each day from reservoir inflows (direct precipitation, upstream and lateral basins flows) and losses (evaporation, lake outflow), where evaporation was estimated with the Rohwer's equation (Rohwer, 1931).

### 4.2 Downscaling models

#### 4.2.1 The dynamical downscaling model MAR

The Modèle Atmosphérique Régional (MAR; Gallée, 1995; Gallée and Schayes, 1994; Gallée et al., 1996) is a hydrostatic primitive equation model for regional atmospheric simulations. It includes a detailed scheme of clouds microphysics with

https://doi.org/10.5194/hess-2023-92
Preprint. Discussion started: 20 April 2023


Hydrology and Earth System Sciences
Discussions

six prognostic equations for specific humidity, cloud droplet concentration, cloud ice crystals (concentration and number), concentration of precipitating snow particles and rain drops. The convective adjustment is parameterized according to Bechtold et al. (2001). MAR is coupled to the one-dimensional land surface scheme SISVAT (Soil Ice Snow Vegetation Atmosphere Transfer; De Ridder and Schayes, 1997; Gallée et al., 2001) that includes a snow multilayer scheme (Brun et al., 1992; Gallée and Duynkerke, 1997).

First designed for polar regions, especially Antarctica and Greenland (e.g. Gallée et al., 1996), MAR was also applied over other regions worldwide, such as midlatitudes areas (e.g. Wyard et al., 2017; Doutreloup et al., 2019), mountainous areas (e.g. Himalaya, Ménégoz et al., 2013) and West Africa (e.g. Chagnaud et al., 2020). For the present study, we use MAR simulation forced by the ERA-20C reanalysis over 1902-2009 and produced at a 7 km resolution over the European Alps (Ménégoz et al., 2020; Beaumet et al., 2021). The URR catchment is covered by 281 MAR grid points.

#### 4.2.2 The statistical downscaling model SCAMP

SCAMP (Sequential Constructive Atmospheric Analogues for Multivariate weather Predictions; Raynaud et al., 2020) is a statistical downscaling model based on atmospheric analogues (Lorenz, 1969). It assumes that similar large-scale atmospheric configurations lead to similar local or regional weather situations (e.g. Obled et al., 2002; Chardon et al., 2014). The simulation process is partly stochastic: for each simulation day, one of the 30-nearest analogues is randomly selected and used as weather scenario for this day. SCAMP can thus be used to generate multiple weather scenarios. In the present work, SCAMP was used to generate 30 time series of daily spatial weather scenarios for the 1902-2009 period from ERA-20C reanalysis outputs. The simulation process is described in the following and summarized in Fig. 3.

(1) For each day of the simulation period, the 30-nearest atmospheric analogue days are identified from candidate days available in the archive period (1961-2009 in the present case). The candidate days are the days found within a 61-days calendar window centered on the target day. A two-step analogue selection is considered. The 100-nearest analogues in terms of large-scale atmospheric circulation are first identified. The selection criterion is the Teweles-Wobus Score (Teweles and Wobus, 1954) applied to the daily geopotential heights at 1000 and 500 $\mathrm{hPa}$. It quantifies the similarity between fields from their shapes, informing thus on the origin of air masses. The 30-nearest analogs are sub-selected from those 100-nearest analogs, based on small-scale atmospheric features following Raynaud et al. (2020) (namely 600 $\mathrm{hPa}$ vertical velocities and large-scale temperature at 2 $\mathrm{m}$ from September to May, large-scale precipitation otherwise).

(2) Following Chardon et al. (2016), SCAMP is used to generate MAP and MAT values for the whole URR catchment. To generate weather scenarios with values different from observations, SCAMP extends the analogue method with a random generation process from a day-to-day adjusted statistical distribution (Chardon et al., 2018; Raynaud et al., 2020). For precipitation, a Gamma distribution is fitted each day to the 30 regional MAP values obtained for the whole URR catchment from the analogues. The distribution is then used to generate a new sample of 30 regional MAP values, thus unobserved (and possibly higher than observations). This adaptation was shown to improve the simulation of maximum regional MAP accumulations (Raynaud et al., 2020, Fig. 8 therein).

https://doi.org/10.5194/hess-2023-92
Preprint. Discussion started: 20 April 2023


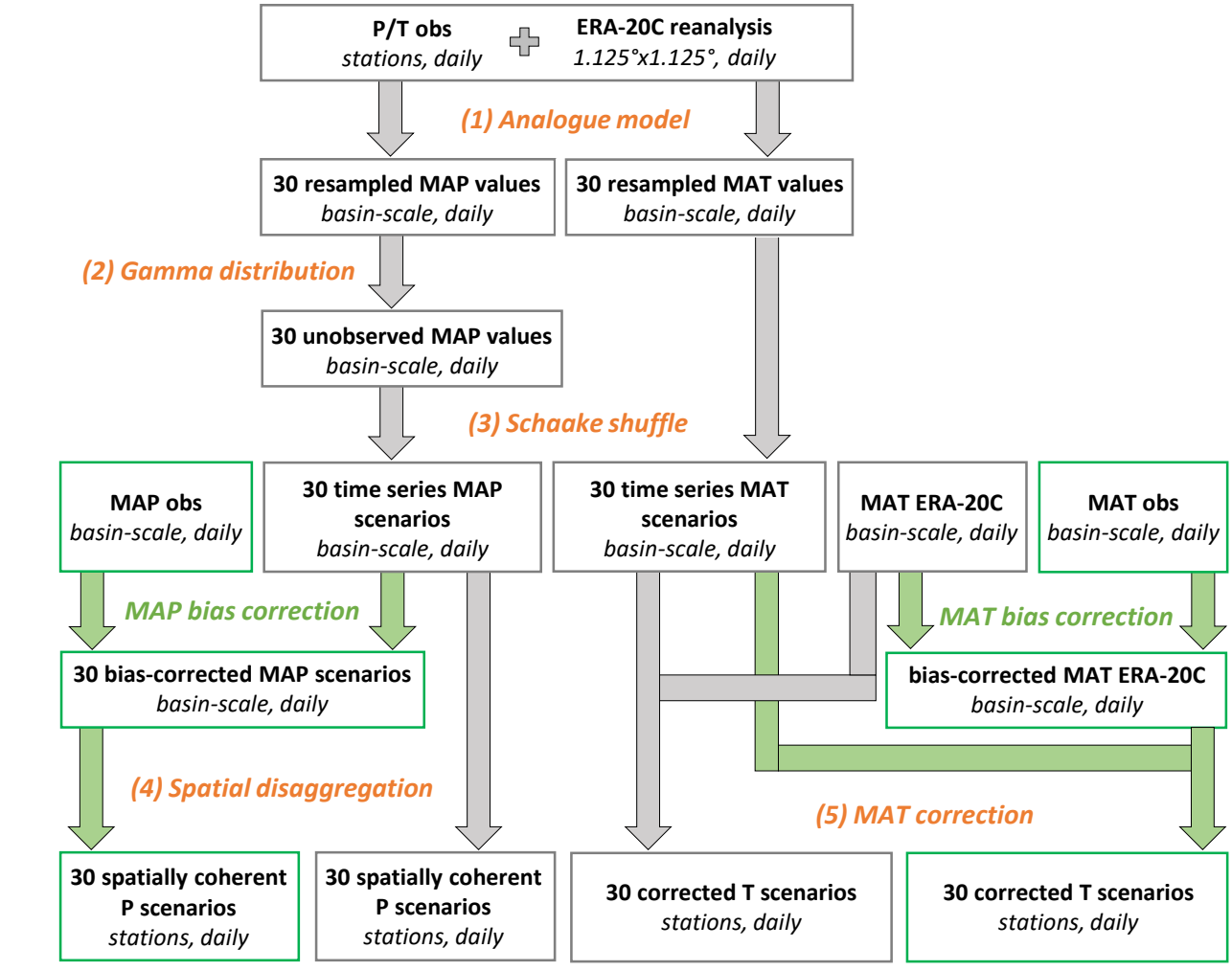


**Figure 3.** Scheme of the statistical downscaling model SCAMP. (**orange**) Components used in the SCAMP simulation. (**green**) Additional components used in the SCAMP bias-corrected simulation. (**bold**) Outputs obtained after each step. (**italics**) Spatial and temporal resolutions.

(3) 30 regional MAP and MAT time series are produced from the 30 regional MAP and MAT values generated each day. To improve the temporal consistency between consecutive days in each time series, the 30 regional MAP and MAT scenarios obtained for each day are paired with those of previous days with a Schaake shuffle reordering approach (Clark et al., 2004; Raynaud et al., 2020).

(4) Following Mezghani and Hingray (2009) and Viviroli et al. (2022), the regional MAP time series are finally disaggregated with a non-parametric method of fragment to produce spatial MAP scenarios for the URR catchment (with one MAP value for each RHHU of the hydrological model).

https://doi.org/10.5194/hess-2023-92
Preprint. Discussion started: 20 April 2023


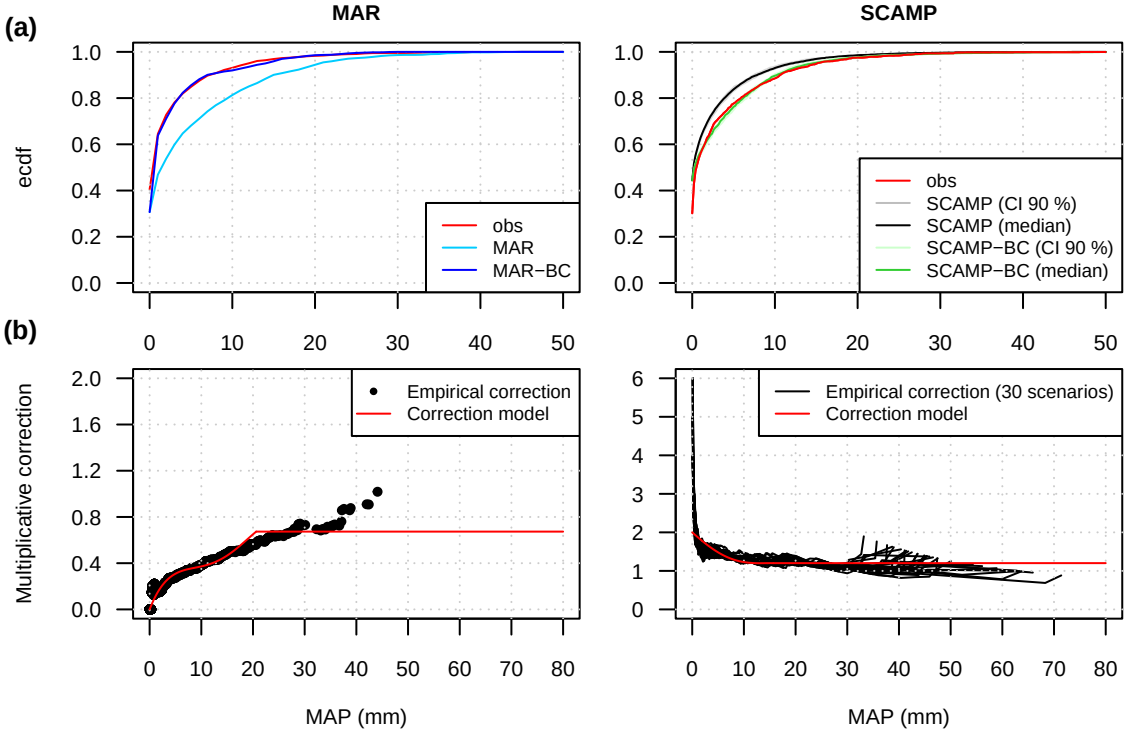


**Figure 4.** Examples of bias correction for regional MAP. MAR: sub-basins 1 to 4, January. SCAMP: whole catchment, August. Control period: 1961-2009. (**a**) empirical cumulative distribution functions (ecdf). (**b**) Correction functions. For SCAMP, the grey and green bands represent the confidence interval at 90 % level. The median scenarios are indicated by the black and green solid lines.

(5) The large-scale atmospheric features considered for the identification of the analogues are not as informative for temperatures. The temperature additive correction method of Kuentz et al. (2015) was thus used to make each day the regional MAT scenarios coherent with the regional MAT configuration of the ERA-20C reanalysis. For each prediction day and each scenario, the correction factor is the difference between the regional MAT value of the ERA-20C reanalysis and the regional MAT value of the scenario. The correction factor is applied to correct the temperature of all stations for this scenario. For instance, if the daily regional MAT value of the scenario is 2 °C warmer than the regional MAT value of the ERA-20C reanalysis, then all local temperatures of the scenario are lowered by 2 °C.

### 4.3 Bias correction

As shown later, simulated weather scenarios from both MAR and SCAMP can be significantly different from observations. Corrected precipitation and temperature scenarios were also considered in the following. A quantile mapping bias correction (BC hereafter) was used for both variables and both models (Déqué, 2007). The different regional MAP and MAT time series

https://doi.org/10.5194/hess-2023-92
Preprint. Discussion started: 20 April 2023


Hydrology and Earth System Sciences
Discussions

were corrected using the observed regional MAP and MAT time series as references. As commonly done, the correction is additive for MAT and multiplicative for MAP, and one BC function was estimated for each calendar month respectively.

To keep the small-scale variability between the different scenarios produced by SCAMP, one single BC function is considered for the 30 time series. An analytical BC function is used to ease interpolations of correction factors estimated between empirical percentiles (a degree 4 polynomial is fitted to the empirical correction factors). To avoid non relevant extrapolations of correction factors for extreme precipitation values non simulated in the control period, the correction value was also bounded. It was bounded for the highest precipitation percentiles (95 to 100 percentiles) to their mean empirical correction value. For temperature, the corrections for the lowest (0 to 5) and for the highest percentiles (95 to 100) were similarly set to their mean empirical correction values respectively.

For SCAMP, the MAP and MAT corrections can only be performed at the scale of the whole catchment. For MAR, a specific BC was applied for each of the 5 major sub-basins of the system (Fig. 1). Examples of BC functions are shown for MAP in Fig. 4. Note that for the dynamical downscaling, a BC of the temperature lapse rate was also necessary. This point is further discussed in Sect. 6.2.

### 4.4 Experimental setup

Four experiments are considered in the present work. They are summarized in Fig. 5. Weather scenarios are produced with either the MAR model or the SCAMP model from large-scale atmospheric information (ERA-20C data). Weather scenarios obtained with each downscaling model are used to force the GSM-SOCONT model and simulate hydrological scenarios. Weather scenarios are first used with their raw values and then with bias-corrected values. In the following, simulations with raw weather scenarios are referred to as "MAR" and "SCAMP" simulations. Bias-corrected simulations are referred to as "MAR-BC" and "SCAMP-BC" simulations. Both weather and hydrological scenarios can be compared to their counterpart references (observed or simulated as explained below). Among other things, we will compare the ability of each hydro-meteorological simulation chain to reproduce the day–to-day temporal variations of both weather variables and discharges.

As many sub-basins have altered hydrological regimes, the "hydrological reference" used for the comparison is the discharge time series obtained via hydrological simulation with the "observed weather" as input. For some upstream sub-basins, which hydrological behavior can be considered as roughly natural, the evaluation could also rely on a comparison with discharge observations. We however choose to use the simulated reference. This first makes the evaluation homogeneous for all URR sub-basins. This additionally allows to only focus on the ability of downscaling chains to simulate hydrologically relevant weather scenarios. In other words, this allows to not distort the evaluation by intrinsic errors introduced by the hydrological model.

A multi-scale evaluation of simulations has been carried out. We here present the meteorological evaluations carried out at the scale of the 5 major sub-basins shown in Fig. 1 and hydrological evaluations at 4 illustrative gauging stations. Rhône@Porte-du-Scex $\left(\text{gauged area of } 5,390\,\mathrm{km}^2\right)$ is the outlet to Lake Geneva of the upstream part of the catchment. Rhône@Genève, Halle-de-l'Ile $\left(7,945\,\mathrm{km}^2\right)$ is the outlet of Lake Geneva. Arve@Genève, Bout-du-Monde is on the Arve River before its

https://doi.org/10.5194/hess-2023-92
Preprint. Discussion started: 20 April 2023


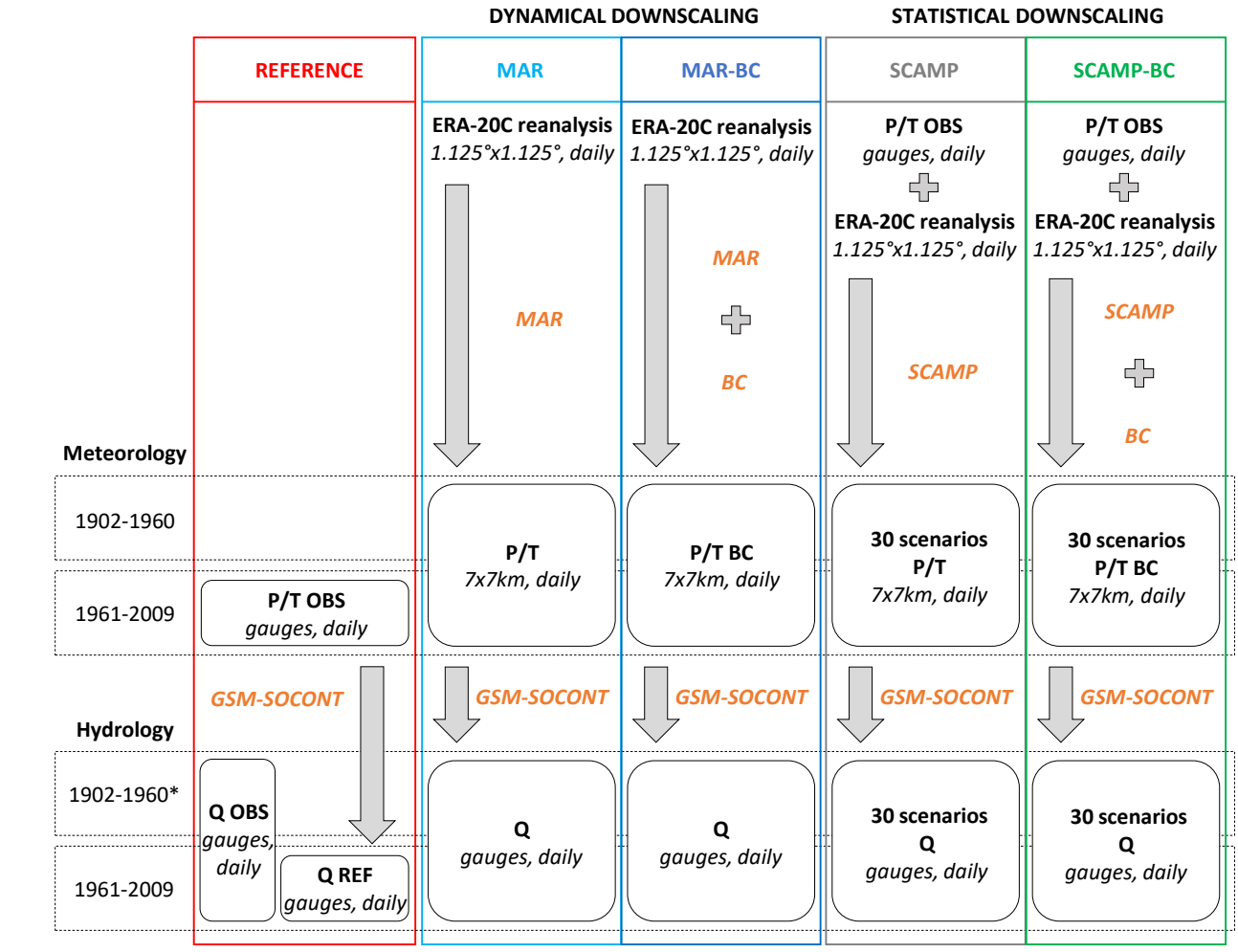


**Figure 5.** Summary of the different experiments. (**orange**) Models used. (**bold**) Outputs obtained after each step. (**italics**) Spatial and temporal resolutions. (*) Time period depending on the considered gauge.

confluence with the Rhône River $(1,990\,\mathrm{km}^2)$, and Rhône@Bognes $(10,900\,\mathrm{km}^2)$ is the most downstream location of the system.

## 5 Results

### 5.1 Weather

Simulated weather variables are compared to observations in Fig. 6 and 7 for both downscaling models. Figure 6 shows observed and simulated year-to-year variations of annual MAP and MAT and Fig. 7 the seasonal cycles of monthly MAP and

https://doi.org/10.5194/hess-2023-92
Preprint. Discussion started: 20 April 2023


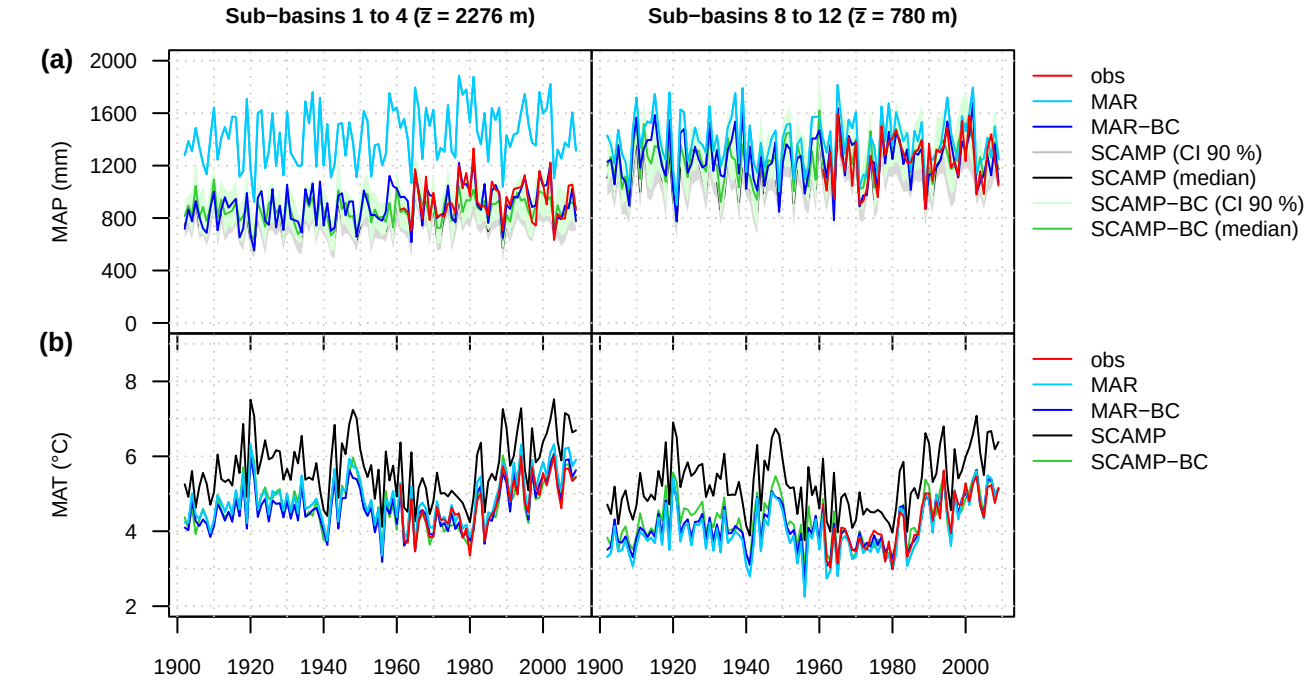


**Figure 6.** Time series of annual (**a**) MAP and (**b**) MAT for two major basins (1902-2009). The average elevation of each major basin is indicated in brackets. For MAP, the grey and green bands represent the confidence interval at 90 % level. The median scenarios are indicated by the black and green solid lines. For MAT, the 30 SCAMP scenarios are identical and both correspond to the raw or to the BC annual time series of the ERA-20C reanalysis.

MAT. Results are presented for sub-basins in the upper part of the URR catchment (sub-basins 1 to 4, Fig. 6 and 7, left) and for sub-basins downstream and around Lake Geneva (sub-basins 8 to 12, Fig. 6 and 7, right). For SCAMP, both figures present the dispersion between the 30 annual MAP values obtained from the 30 time series scenarios (grey and green bands). Note that the dispersion is rather large for precipitation (e.g. up to 600 mm for annual MAP, Fig. 6), illustrating the important uncertainty in the large-scale-small-scale relationship for this variable in this region.

For both downscaling models, simulated year-to-year variations of regional annual MAP and MAT are in good agreement with observed ones, whatever the area considered (Fig. 6). The positive trend in temperature starting in 1980 is also adequately reproduced. However, mean simulated variables can be rather different than observed ones. For MAR for instance (cyan lines), simulated annual MAP are 12 % higher than observations for sub-basins around the lake and 58 % higher for sub-basins in the upper part of the URR catchment. For SCAMP (grey bands and black lines), the differences, although much smaller, are still significant: depending on the SCAMP scenario, simulated annual MAP are 2 % to 8 % smaller than observations around the lake and 10 % to 15 % smaller for the upper part of the URR catchment. Some differences are also obtained for annual MAT.

https://doi.org/10.5194/hess-2023-92
Preprint. Discussion started: 20 April 2023


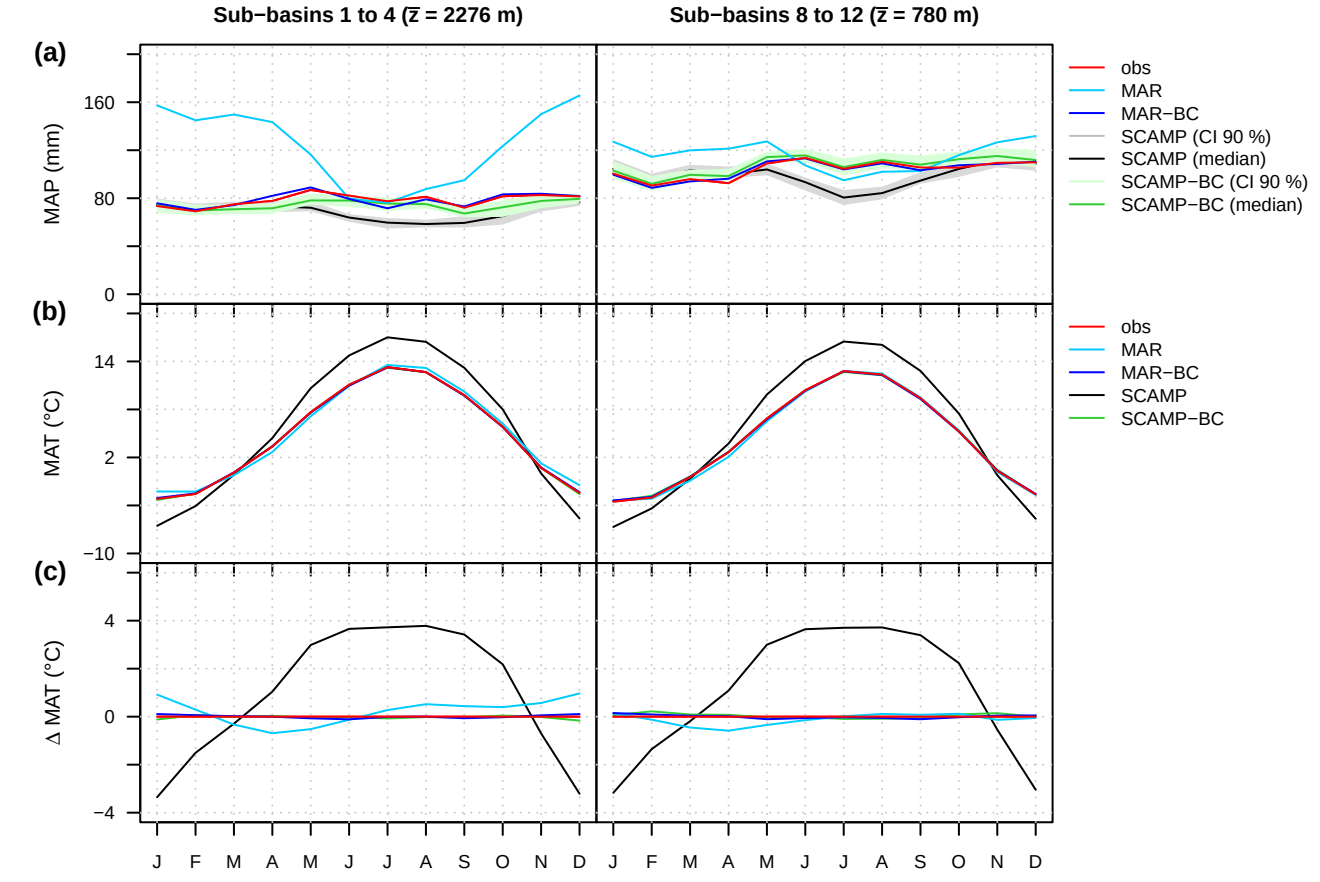


**Figure 7.** Seasonal cycles of (**a**) MAP and (**b**, **c**) MAT for two major basins (1961-2009). The average elevation of each major basin is indicated in brackets. For MAP, the grey and green bands represent the confidence interval at 90 % level. The median scenarios are indicated by the black and green solid lines. For MAT, the 30 SCAMP scenarios are identical and both correspond to the raw or to the BC seasonal cycle of the ERA-20C reanalysis.

They are small for MAR (0.1 °C around the lake, 0.3 °C in the upper part of the URR catchment). For SCAMP, simulations are roughly 1 °C warmer for the whole area (black lines).

As shown in Fig. 7, deviations from observations can vary a lot from one season to another. In the upper part of the URR catchment, precipitation amounts simulated with MAR are similar to observations in summer but much larger in fall and spring (resp. +56 % and +71 %) and even larger in winter (+110 %). Around the lake, simulated precipitations are almost similar to observations in fall (+8 %) and summer (-7 %) but are again significantly larger in winter and spring (+24 %). For SCAMP scenarios, differences are almost exclusively found in summer when simulated MAP are 15 % to 30 % smaller than the observations for the whole area. A significant seasonality of deviations is also found for MAT. For MAR, the difference is

https://doi.org/10.5194/hess-2023-92
Preprint. Discussion started: 20 April 2023


Hydrology and Earth System Sciences
Discussions

315 -0.7 °C in spring and up to +1.1 °C in winter. For SCAMP, the seasonality is even larger: simulations are up to 3.7 °C warmer than observations in summer and conversely up to 2.7 °C colder in winter.

For both models, the differences mentioned above are significantly reduced and sometimes vanish completely after BC (blue lines for MAR-BC and green bands/solid lines for SCAMP-BC). This is the case for annual variables (Fig. 6) but also for monthly variables (Fig. 7) as the BC is performed on a monthly basis. For SCAMP, as BC is performed at the catchment-scale,
320 some biases can remain at the sub-catchment scale. For annual MAP for instance, simulations are still 3 % to 9 % smaller than observations in the upper part of the URR catchment and 0 % to 6 % larger around the lake depending on the scenario (Fig. 6).

### 5.2 Discharge seasonality and variations

The discharges obtained via hydrological simulation from weather scenarios are compared with their reference counterparts, i.e. with the discharges obtained via hydrological simulation from observed weather variables. The comparison was applied
325 to time series of discharges at daily, monthly and annual resolutions, and to time series of characteristic discharge variables (i.e. minimum monthly discharge observed each year and annual maximum daily discharge). Results presented here only cover parts of our comparisons. Note that for SCAMP and SCAMP-BC simulations, for which 30 time series scenarios are simulated, the value of the reference discharge variable considered for a given time is compared to the 30 values obtained for that time from the 30 scenarios respectively.

330 At a daily time step, the discharge time series of MAR-BC and SCAMP-BC simulations are in good agreement with the reference ones as shown with results obtained for the four illustrative gauging stations in Fig. 8. The agreement is even larger for time series of mean monthly discharges (Fig. 10, left). The large seasonality of flows but also the temporal variations (day-to-day variations, monthly variations) of flows is well reproduced, especially for the Rhône River upstream of Lake Geneva. These results are obtained for almost all gauging stations, even for stations downstream of Lake Geneva despite the significant
335 influence of the lake regulation on flows and the rather crude regulation model used for its representation (Fig. 8e).

For both downscaling models, BC of weather scenarios significantly improves simulations (Fig. 8 versus Fig. 9). BC is actually required for both precipitation and temperature variables. This is especially visible with results obtained for the upstream URR catchment. At Rhône@Porte-du-Scex (Fig. 9a), discharge variations are rather well reproduced with raw weather scenarios but discharges are overestimated with SCAMP and underestimated with MAR during the spring and summer. These
340 deviations may be surprising as raw SCAMP and MAR precipitation simulations are biased toward not enough summer precipitation in SCAMP and conversely much larger winter, spring and fall precipitation in MAR (Fig. 7). They actually derive from temperature scenarios which are too warm in SCAMP in summer and not warm enough in MAR. This point is further discussed in Sect. 6.2.

### 5.3 Flood events and low flow sequences

345 The hydrological relevance of simulated weather scenarios is further evaluated with simulations of low flow sequences and flood events. Figure 10 (middle, right) presents scatter plots of simulated and reference values of annual monthly low flows and annual daily floods obtained for the 49 years of the 1961-2009 period. The same figure with results for the first half of the

https://doi.org/10.5194/hess-2023-92
Preprint. Discussion started: 20 April 2023


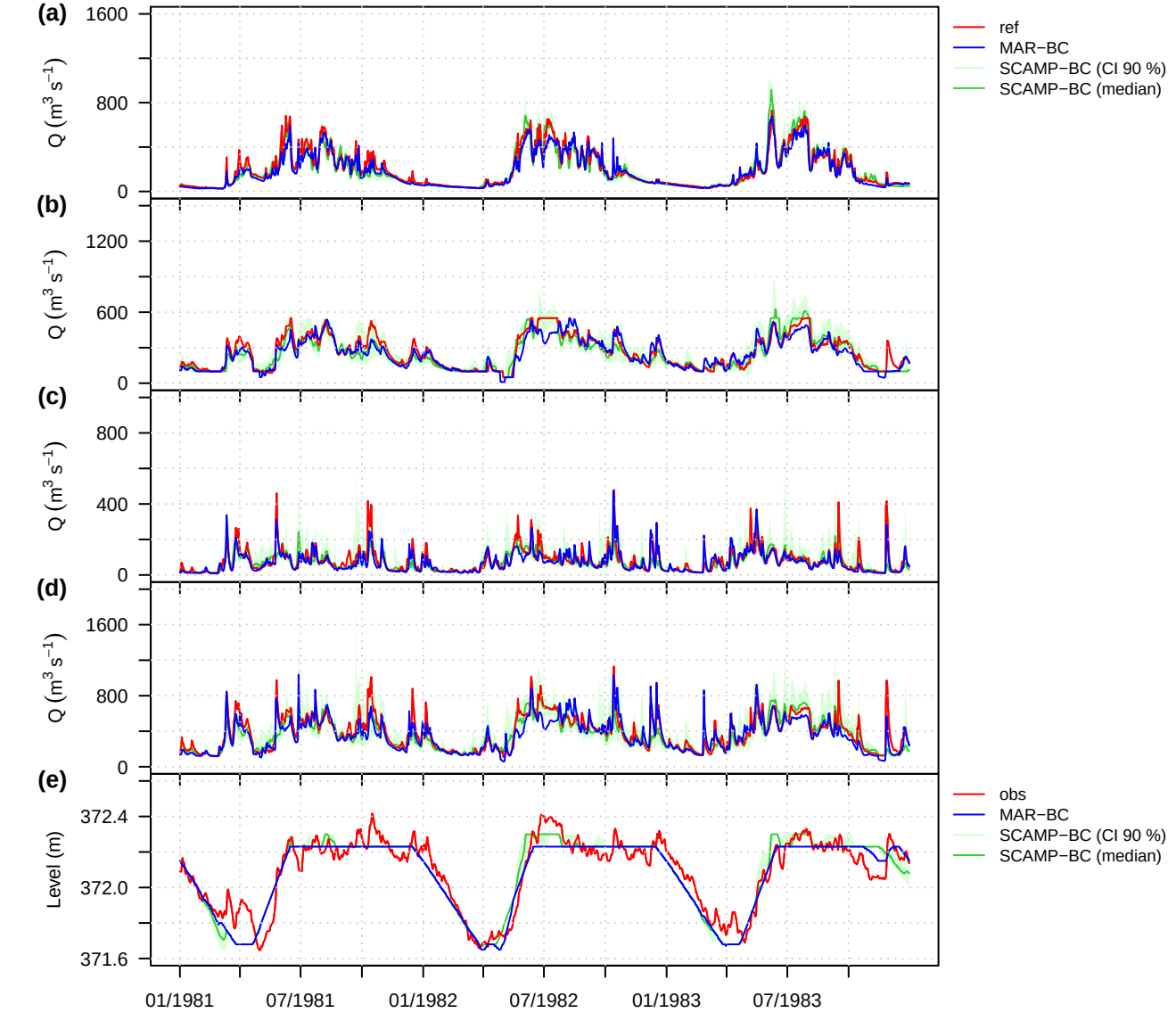


**Figure 8.** Time series of daily discharges at (**a**) Rhône@Porte-du-Scex, (**b**) Rhône@Genève, Halle-de-l'Ile, (**c**) Arve@Genève, Bout-du-Monde, (**d**) Rhône@Bognes for the 1981-1983 period. (**e**) Time series of daily level of Lake Geneva for the same period. The green bands represent the confidence interval at 90 % level. The median scenarios are indicated by the green solid lines.

century is given in Supplementary Materials (Fig. S3). For low flows, the month with the lowest monthly flow in the reference discharge series is identified for each year of the period. The 49 lowest monthly low flows are compared to their simulated counterparts for the same months. For flood events, a similar comparison is made: for each year, the day with the highest reference daily flow is identified, and the corresponding discharge is compared to the maximum daily discharges obtained

https://doi.org/10.5194/hess-2023-92
Preprint. Discussion started: 20 April 2023


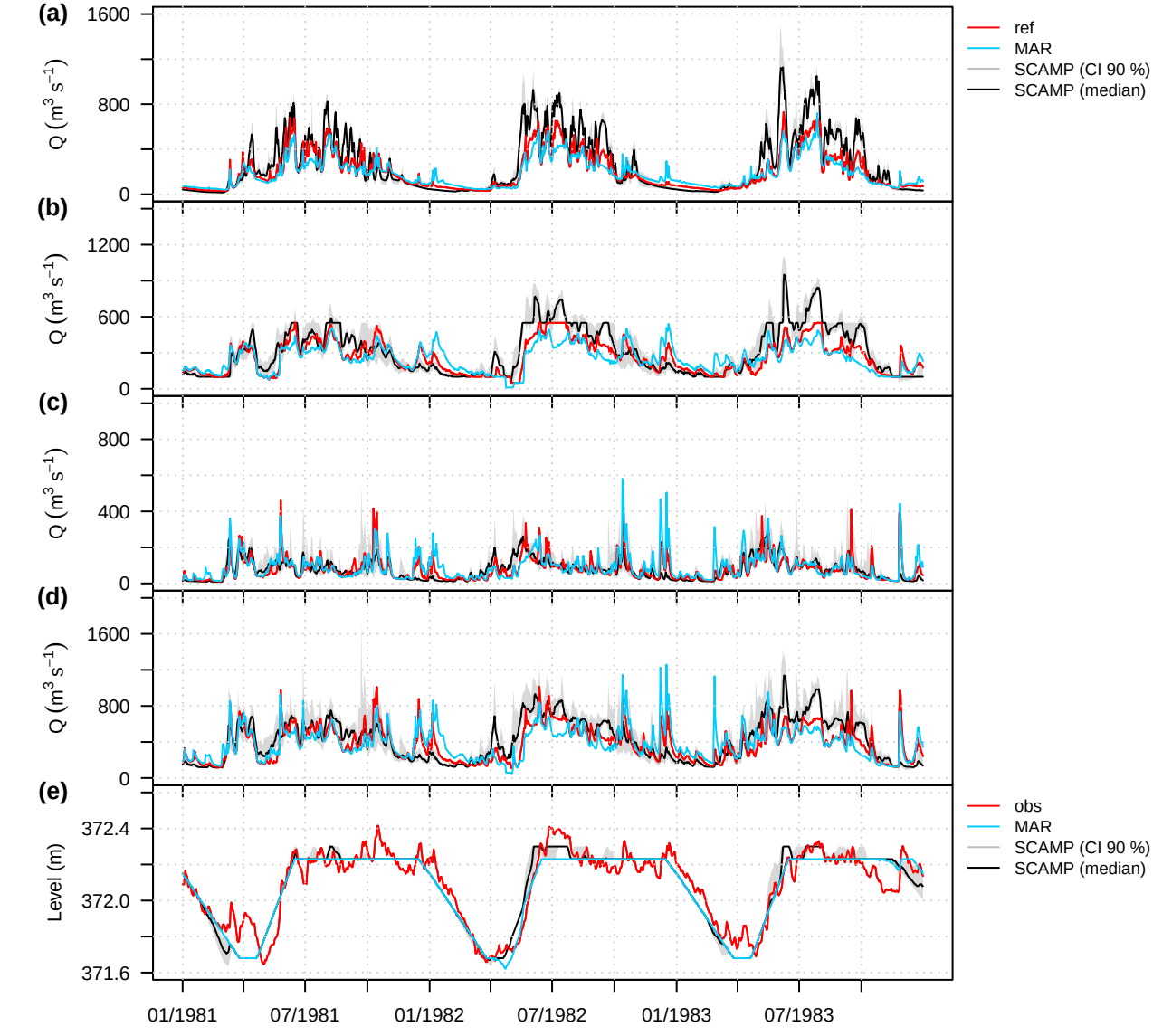


**Figure 9.** Time series of daily discharges at (**a**) Rhône@Porte-du-Scex, (**b**) Rhône@Genève, Halle-de-l'Ile, (**c**) Arve@Genève, Bout-du-Monde, (**d**) Rhône@Bognes for the 1981-1983 period. (**e**) Time series of daily level of Lake Geneva for the same period. The grey bands represent the confidence interval at 90 % level. The median scenarios are indicated by the black solid lines.

around that day in the simulations (the maximum discharge considered for the comparison in the simulation is identified from a 7-day window centered on the reference day).

For all gauging stations, the MAR-BC simulation leads to very satisfactory results for low flows. By contrast, flood events tend to be underestimated (at Rhône@Porte-du-Scex, Rhône@Genève, Halle-de-l'Ile and Rhône@Bognes) or poorly simulated

https://doi.org/10.5194/hess-2023-92
Preprint. Discussion started: 20 April 2023


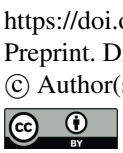

Hydrology and Earth System Sciences
Discussions
Open Access
EGU

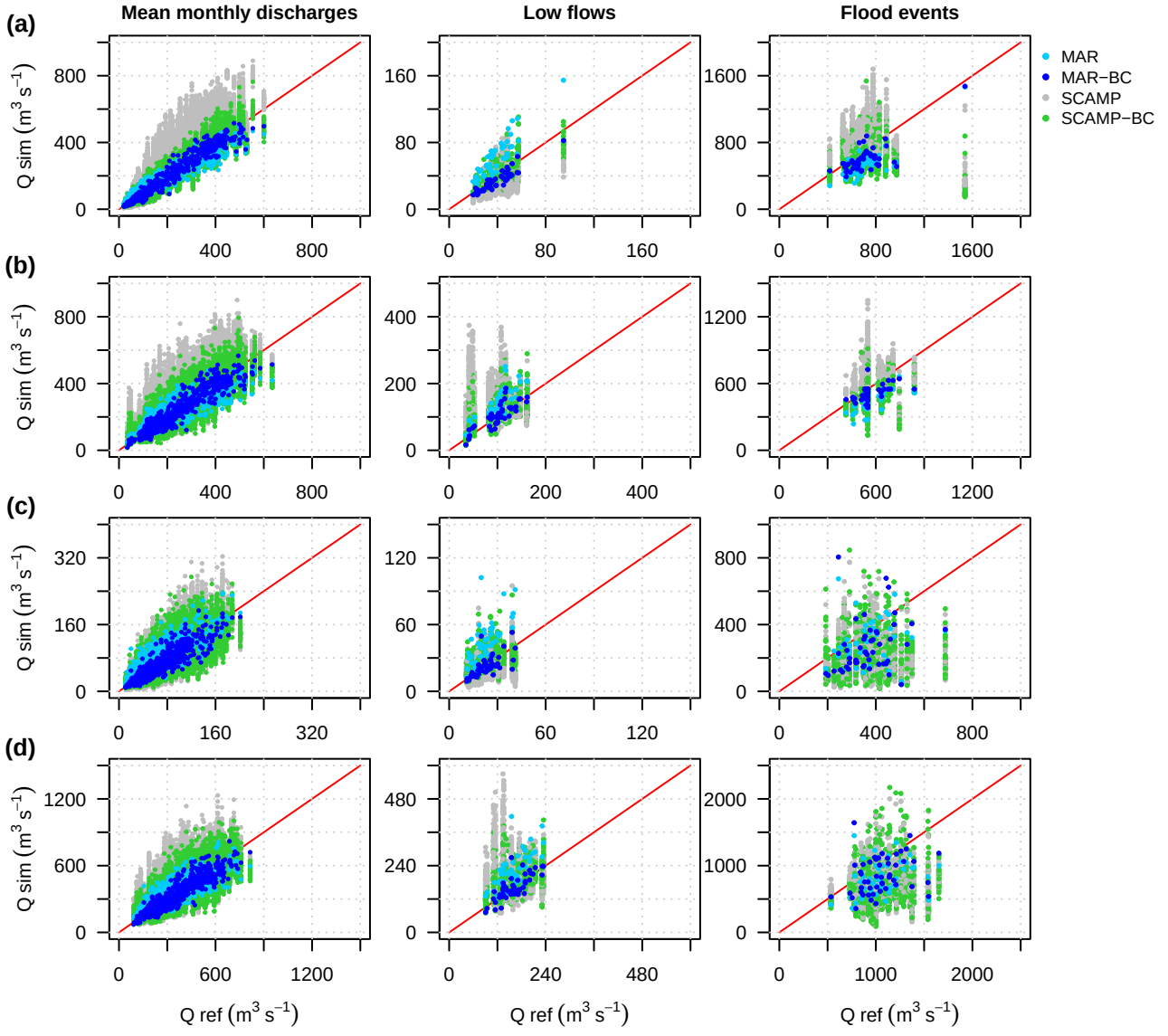


**Figure 10.** Scatter plots of mean monthly discharges, low flows and flood events at (**a**) Rhône@Porte-du-Scex, (**b**) Rhône@Genève, Halle-de-l'Ile, (**c**) Arve@Genève, Bout-du-Monde, and (**d**) Rhône@Bognes for the 1961-2009 period. See text for definitions of low flows and flood events.

(at Arve@Genève, Bout-du Monde). For SCAMP-BC simulations, the low flows and flood events are characterized by a very large inter-scenario variability, making the interpretation of these results more difficult. For low flows, the medians of simulated scenarios are close to the reference ones at all gauging stations. For flood events, the medians are also close to the reference values at Rhône@Porte-du-Scex. They are however off center downwards at Rhône@Genève, Halle-de-l'Ile and at the two

https://doi.org/10.5194/hess-2023-92
Preprint. Discussion started: 20 April 2023


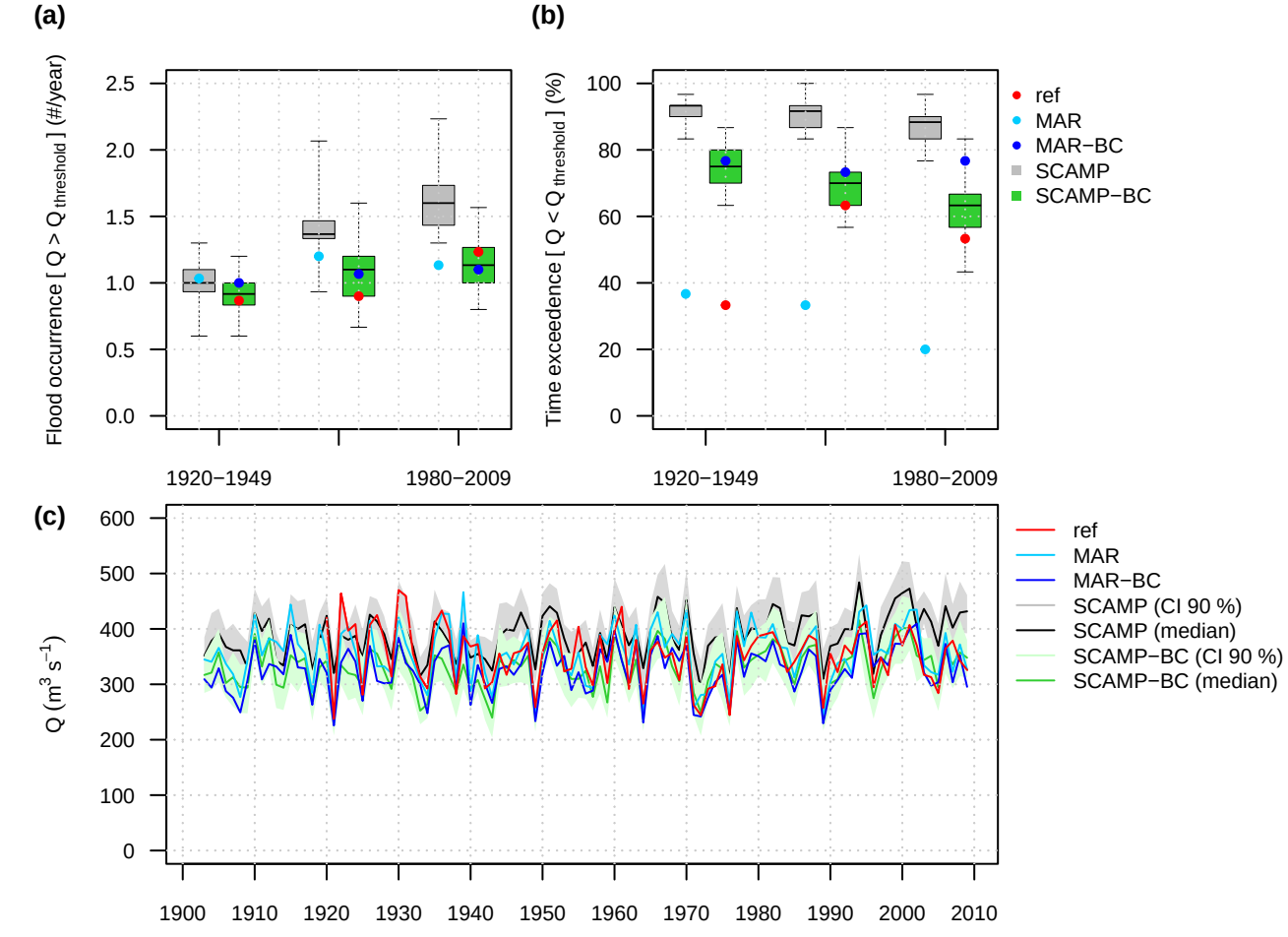


**Figure 11.** (**a**) Flood activity and (**b**) low flow activity at Rhône@Bognes for three 30-year sub-periods: 1920-1949, 1950-1979 and 1980-2009. See text for definitions of flood activity and low flow activity. (**c**) Mean annual discharge at Rhône@Bognes for the period 1902-2009. The grey and green bands represent the confidence interval at 90 % level. The median scenarios are indicated by the black and green solid lines.

stations on the Rhône River downstream of Lake Geneva. The least well reproduced flood events are those of the Arve basin and those at Rhône@Bognes. Conversely to the upper part of the URR catchment, these floods occur mainly in late summer and fall (see Fig. S4 in Supplementary Materials). MAR-BC and SCAMP-BC simulations may thus fail to reproduce the large rainfall amounts in that season, especially convective events, known to generate the largest fall floods in this area.

### 5.4 Mean annual discharges, flood and low flow activities

The simulation chains considered previously are typically used for hydroclimatic projections with large-scale atmospheric outputs of GCM as forcing variables. The potential impact of climate change on hydrology is often assessed considering

https://doi.org/10.5194/hess-2023-92
Preprint. Discussion started: 20 April 2023


Hydrology and Earth System Sciences
Discussions

changes in the statistical characteristics of hydrological regimes, for instance changes in seasonality and year-to-year variability, changes in flood and low flow activities, etc. We therefore also assess the ability of the considered simulation chains to simulate the observed variations of different hydrological regime features over the last 100 years.

We first consider variations of flood and low flow activities of the URR catchment. Flood activity is here defined as the number of flood events within a 30-year period exceeding a given discharge threshold. Low flow activity is similarly defined as the number of months within a 30-year period for which the mean monthly discharge is below a given discharge threshold. The thresholds retained are the discharge values exceeded in average one time per year on the entire 90-year simulation period 1920-2009. At Rhône@Bognes, the thresholds are respectively 962 $\mathrm{m}^3\ \mathrm{s}^{-1}$ for floods and 162 $\mathrm{m}^3\ \mathrm{s}^{-1}$ for low flows. The flood and low flow activities, estimated for each of the three 30-year sub-periods 1920-1949, 1950-1979 and 1980-2009, are presented in Fig. 11 (a, b).

The number of flood events exceeding the threshold in the MAR-BC and SCAMP-BC simulations as well as the variations of flood activity from one sub-period to another are in good agreement with the reference ones (Fig. 11a). The results for low flow activity are less satisfactory, especially for the 1920-1949 sub-period (Fig. 11b). The number of low flow sequences below the threshold in both simulations is indeed twice that of the reference. This suggests a limitation of both downscaling models to simulate long persistent dry sequences.

Simulated year-to-year variations of mean annual discharges are next compared to the "reference" ones over the 1920-2009 period (Fig. 11c). The "references" are observed discharges for the 1920-1960 period and simulated discharges from observed weather for the 1961-2009 period. Because of the large interannual variability of discharges, it would be rather difficult to assess the ability of the chains to catch possible long term trends of this variable. However, the year-to-year variations are well reproduced in both timing and amplitude especially for the second half of the century (recall especially that the hydrological model does not alter the comparison during this sub-period as both time series compared are obtained by hydrological simulation).

## 6 Discussion

All in all, and as already illustrated in some previous works (e.g. Boé et al., 2007; Kuentz et al., 2015; Caillouet et al., 2017), hydrologically relevant weather scenarios (or reconstructions) can be achieved with either statistical or dynamical downscaling models from large-scale atmospheric information only. As illustrated here also, this may require some preliminary BC to atmospheric model outputs.

As discussed in the following, the need for corrections can be attributed to some limitations of the models. It may be also attributed to the quality of available "observations". We will discuss issues related to reanalysis data and to lapse rates for both temperature and precipitation.

https://doi.org/10.5194/hess-2023-92
Preprint. Discussion started: 20 April 2023


Hydrology and Earth System Sciences
Discussions

### 6.1 Reanalysis data

The ERA-20C reanalysis considered for this study is used as pseudo-observation of the atmospheric state and dynamics over a large spatial area covering the European domain. It is however produced by assimilation of sea level pressure and wind measurements only. The quality of the geopotential at 500 $\mathrm{hPa}$ and of the other large-scale variables (like 600 $\mathrm{hPa}$ vertical velocities, temperature at 2 $\mathrm{m}$, large-scale precipitation, etc) may be therefore rather low for some variables and may impact the skill of both downscaling models.

This is for instance the case for the regional MAT value used to force the SCAMP scenarios. The large bias in the regional MAT SCAMP scenarios highlighted in Fig. 6 and 7 directly derives from the bias of the regional MAT of the ERA-20C reanalysis over the considered domain. As shown by Horton and Brönnimann (2019), using a reanalysis assimilating more data like the recent ERA5 reanalysis (Hersbach et al., 2020) could lead to more relevant weather scenarios. Such reanalyses were not used in the present work because they generally cover a much shorter time period (about 60 years) preventing the simulation and evaluation of hydro-meteorological scenarios over a century.

### 6.2 Temperature lapse rate

For hydrological simulations, MAT estimates are required for each elevation band. They are obtained via interpolation from temperature values available at neighboring stations using a regional elevation-temperature relationship.

For SCAMP simulations, this relationship is estimated each day from the SCAMP temperatures at the stations. For each simulation day, as these temperatures are derived from the temperatures of an observed analog day, the relationship of the scenario always corresponds to an observed one. The elevation-temperature relationship and its variations with time are thus coherent with the observations.

For MAR simulations, this relationship was assumed to be linear and its slope, the so-called "lapse rate", was estimated for each time step from simulated temperatures using all MAR grid cells in the URR catchment. As illustrated in Fig. 12a, the lapse rates estimated from MAR temperatures are in average stronger than those estimated from temperature observations. This likely results from a warm bias in the lower atmospheric layers of the model.

For the mountainous context considered here, this has important implications on the simulated hydrology. A stronger lapse rate leads to lower temperatures than those observed for high elevation bands especially (where few observations are available) and vice versa for low elevation bands. This makes logically the simulated snowpack dynamics significantly different from the observed one. Lower temperatures lead to more frequent solid precipitation, more snow accumulation, less spring snowmelt, presence of a snow cover for longer duration and over larger areas, etc. For the highest elevation bands, lower temperatures can even lead to a perennial simulated snowpack, preventing any ice melt simulation (which can only occur in the model for elevation bands where the glacier is free of snow). All of this results in poorly simulated hydrological regimes, with, for instance, a period of low flow in winter that is too long, a delayed snowmelt flood, too low flows in late summer that are not sustained as they should by ice melt, etc (Fig. 12d). Similarly, flood regimes are expected to be poorly simulated as the fraction of liquid precipitation available for flood generation is probably mis-estimated.

https://doi.org/10.5194/hess-2023-92
Preprint. Discussion started: 20 April 2023


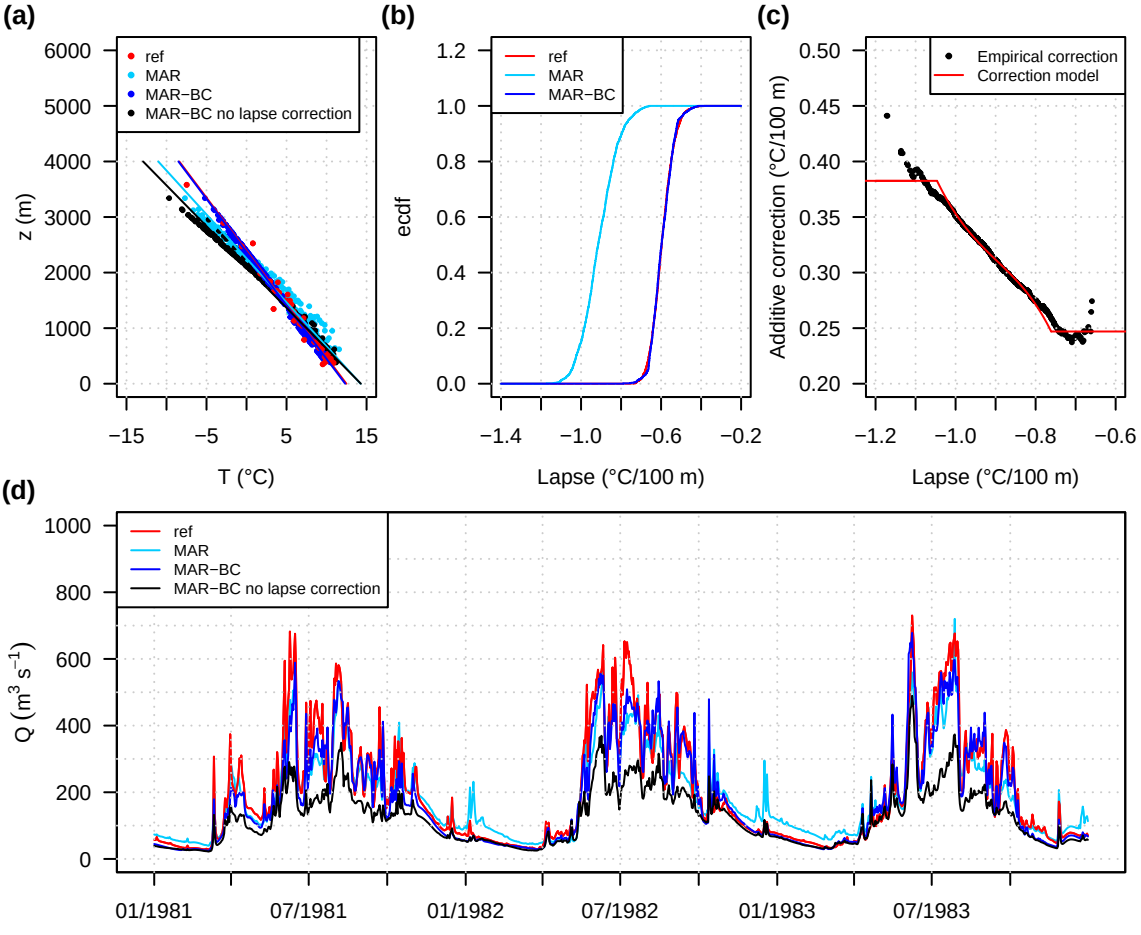


**Figure 12.** (**a**) Elevation-temperature relationship at the catchment-scale. Each point corresponds to the mean temperature over the period 1961-2009 observed at each station (n = 39) or simulated at each grid cell of the model MAR (n = 281). (**b**) and (**c**) Examples of empirical cumulative distribution functions (ecdf) and correction model for temperature lapse rate (sub-basins 1 to 4, July). (**d**) Time series of daily discharges at Rhône@Porte-du-Scex for the 1981-1983 period.

The bias in temperature simulated with RCMs is recognised and corrected for a long time. A common approach to use model temperatures for hydrological simulations is to identify the BC function for a given reference altitude $z_{ref}$ and to use this function to correct model temperatures for all other elevations. In this process however, the model lapse rates remain unchanged and the corrected MAT may still present residual biases for all elevations different from the reference one. This is the case for the present work.

We thus considered here a two-part quantile mapping correction function of MAR temperatures that accounts for both biases, that of the MAT value simulated for a reference elevation and that of the lapse rate. The corrected MAT value for a

https://doi.org/10.5194/hess-2023-92
Preprint. Discussion started: 20 April 2023


Hydrology and Earth System Sciences
Discussions

given elevation $z$ and a given time $t$ is obtained as follows:

$$\mathrm{MAT}_{\text{MAR-BC}}(z,t) = \mathrm{MAT}_{\text{MAR-BC}}(z_{ref},t) + \mathrm{lapse}_{\text{MAR-BC}}(t) \times (z - z_{ref}) \quad (3)$$

where $\mathrm{MAT}_{\text{MAR-BC}}(z_{ref},t)$ is the bias-corrected MAT value at the reference altitude $z_{ref}$ (the correction depends on the percentile of the MAT value at $t$) and $\mathrm{lapse}_{\text{MAR-BC}}(t)$ is the bias-corrected lapse rate value at $t$ (the correction depends on the percentile of the lapse rate value estimated from MAR outputs at $t$).

In practice, we chose the mean altitude of the URR catchment (i.e. 1525 $\mathrm{m}$) as reference altitude. The MAT and lapse rate corrections were carried out independently at the monthly scale and for the 5 major basins shown in Fig. 1. Examples of ecdf and correction functions for MAR lapse rates are shown in Fig. 12 (b, c).

As illustrated in Fig. 12d, the added value of the temperature lapse rate correction for hydrological simulations is definitively large, due to the direct effects of temperature on snow dynamics. To our knowledge, the temperature lapse rate issue was not given a lot of attention in the past, but it likely should more, at least in areas covering large elevation ranges and where highly non linear behaviors with respect to temperature have to be simulated. These results should also lead scientists to integrate this issue when evaluating dynamical downscaling models and to consider appropriate BC approaches before using model outputs to force impact models.

### 6.3 Orographic precipitation enhancement

A similar, but different, issue arises for precipitation. As mentioned above, significant differences are obtained between MAP estimated from downscaled simulations and from observations. This obviously translates directly into significant differences in the simulated hydrology. However, developing relevant MAP estimates is always a challenge in hydrometeorology, especially in mountainous areas (e.g. Ruelland, 2020).

In the present work, the MAP estimated for the reference hydrological simulation were obtained from station observations using the Thiessen's weighting method. For the reasons mentioned in the following, no precipitation-elevation relationship was considered in this estimation. However, annual precipitation generally increases with elevation in the region. Such a dependency is rather clear from observations. It is actually also found in the MAR simulations, even if the simulated precipitation lapse rates may overestimate the true ones (Ménégoz et al., 2020).

The "no precipitation lapse rate" assumption retained for our simulations is thus not really valid. To illustrate the influence of this assumption, we carried out auxiliary "reference" simulations using a constant but elevation-dependant adjustment factor for precipitation (see e.g. Viviroli et al., 2022). In practice, all precipitation data of a given station are multiplied by a constant value, depending on the difference between the elevation of the station and that of the target hydrological unit, before application of the Thiessen weighting process. Two "with precipitation lapse rate" experiments were produced. The adjustment factors were obtained with a linear increase assumption of 5 % and 10 % respectively per 100 $\mathrm{m}$ of elevation.

As shown in Fig. 13, accounting for a precipitation lapse rate has contrasting effects depending on the area considered. It significantly increases the annual MAP estimates for high elevation sub-basins (Fig. 13a, left) but has almost no influence on MAP estimates for low elevation sub-basins (Fig. 13a, right). This reflects the typical under-representation of high elevation

https://doi.org/10.5194/hess-2023-92
Preprint. Discussion started: 20 April 2023


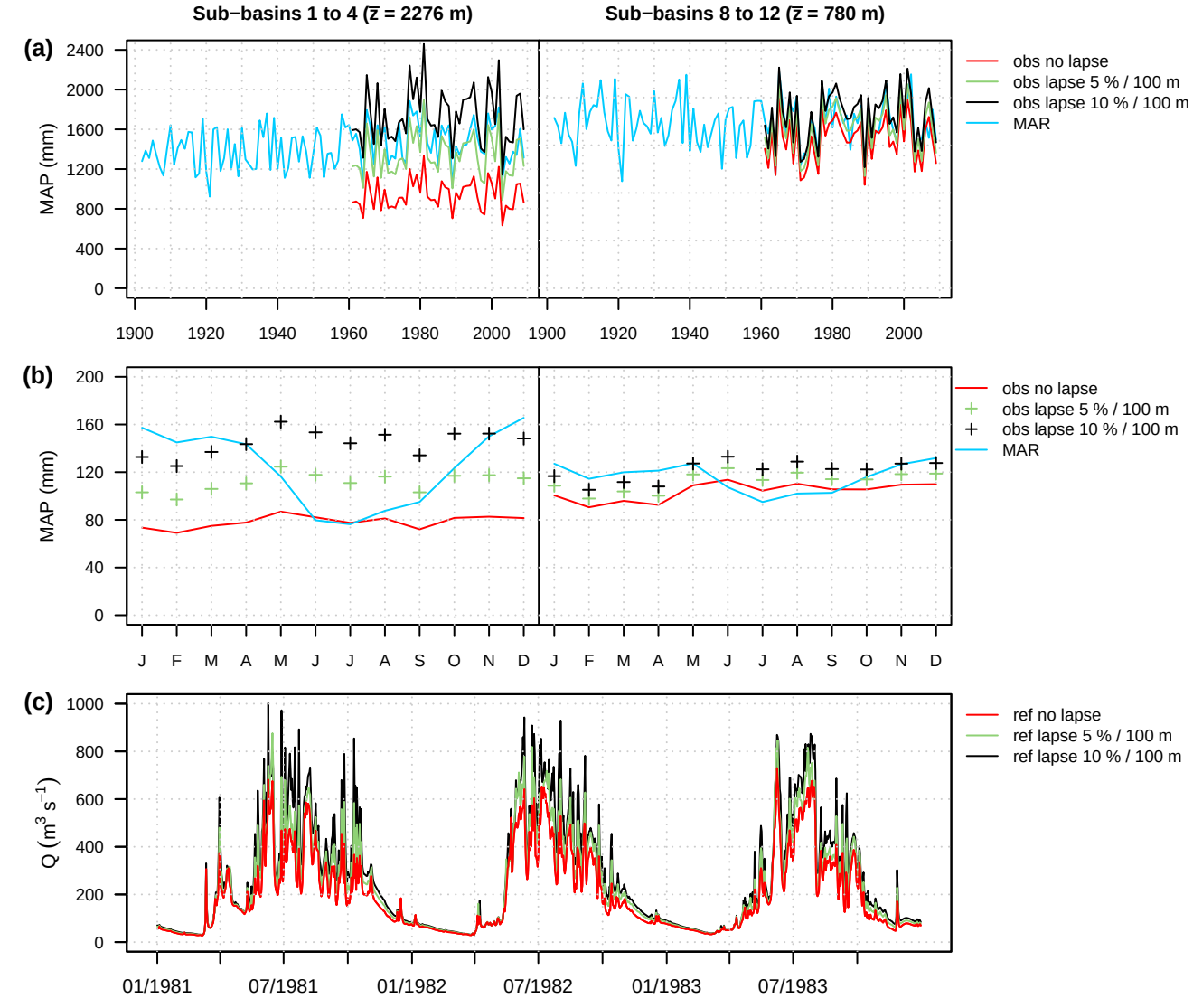


**Figure 13.** Influence of the precipitation lapse rate. (**a**) Time series of annual MAP (1902-2009) and (**b**) seasonal cycles of MAP (1961-2009) for two major basins. The average elevation of each major basin is indicated in brackets. (**c**) Time series of daily discharges at Rhône@Porte-du-Scex for the 1981-1983 period.

stations in the region. All in all, accounting for a precipitation lapse rate significantly reduces the differences between annual amounts from observations and MAR simulations.

For hydrological simulations however, the precipitation-elevation dependency is not trivial to take into account in a relevant way. As shown by Ruelland (2020), if the orographic enhancement can be clearly identified from annual and seasonal means,

https://doi.org/10.5194/hess-2023-92
Preprint. Discussion started: 20 April 2023


Hydrology and Earth System Sciences
Discussions

it is no more obvious at the event-scale, and for any given event, the spatial pattern of precipitation generally depends on where the precipitation event first occurs. This is likely the reason why the precipitation lapse rate is significantly lower in summer than in winter in the region (Fig. 13b), due to much more frequent convective events (e.g. Ménégoz et al., 2020). According to Bárdossy and Pegram (2013), on a daily scale, the orographic effects generally contribute a small part to precipitation variation. In many cases, the orographic enhancement obtained for long accumulation durations is actually often related to more frequent precipitation in high elevations rather than more intense precipitation. Although not verifiable from available observations, this is probably also the case in the region.

Although often determinant, orographic effects cannot be accounted for by a simple and constant adjustment factor, but for practical reasons and lack of better knowledge, this is the usual practice in hydrological modeling. Using a constant adjustment factor for all time steps of a given period however, is likely to have significant and detrimental implications on hydrological simulations. This is particularly likely to amplify in an unrealistic way the largest precipitation events, resulting in turn in huge and unrealistic floods (Hingray et al., 2010). For the URR catchment, hydrological simulations with a precipitation lapse rate produce significantly larger floods (Fig. 13c). With a lapse rate of 5 % / 100 $\mathrm{m}$, the maximum annual floods of the 1961-2009 period are increased by 3 to 106 % (+25 % on average). With a lapse rate of 10 % / 100 $\mathrm{m}$, the increase is even larger (+56 % on average). It is up to 200 % for the largest flood ever observed in the area (15 October 2000) (not shown).

The precipitation-elevation dependency was disregarded in the present work to avoid such unrealistic simulations. This is not really satisfactory, especially regarding the annual water budget of sub-basins. The latter will be mis-represented as a result of the overall dry bias in the precipitation input. Without a better knowledge of how precipitation amounts depend on elevation at the event-scale, disregarding the elevation dependency is probably the best compromise option to choose if relevant flood events have to be simulated. Note that in our simulations, the dry bias in the precipitation input is probably corrected via an adjusted parameterization of the hydrological model, allowing for simulated evapotranspiration losses lower than the actual ones and allowing in turn for the simulation of reasonable discharge time series (parameterization adjustments to correct for imperfect input data are expected to be rather common in the calibration of hydrological models).

## 7 Conclusion

In the present work, two hydro-meteorological modeling chains are used to simulate the past variations of discharge at several stations of the Upper Rhône River basin, a mesoscale basin in the western Alps. Discharges are simulated with the glacio-hydrological GSM-SOCONT model using weather scenarios downscaled with the MAR and SCAMP models from ERA-20C data. MAR is a dynamical downscaling model, SCAMP a statistical one providing an ensemble of downscaled scenarios.

For both chains, given the difficult modeling context of the basin (e.g. unknown effects of the large upstream dams and regulation of Lake Geneva, scarcity of observations for model calibration) and the fact that weather scenarios are only produced from large-scale atmospheric information, simulated discharges are globally in good agreement with the reference ones. For the 1961-2009 period, the multi-scale variations of reference discharges (daily, seasonal and interannual) are well reproduced. To some extent, the simulations also reproduce low flow sequences and annual floods quite well. For the first half of the

https://doi.org/10.5194/hess-2023-92
Preprint. Discussion started: 20 April 2023


century, the agreement with reference discharges is lower (but still reasonable), likely due to lower data quality (ERA-20C and discharges data) and/or to some modeling assumptions and choices (e.g. signature-based calibration, stationarity assumption). Nevertheless, both chains are able to accurately reproduce the variations in flood activity over the last 100 years. The results for low flow activity are less satisfactory.

Both chains are likely to be appropriate for the generation of relevant regional weather scenarios for different climate contexts, from outputs of ad hoc GCM experiments. Thanks to its much lower computational cost, the SCAMP model is to be favored when large ensemble of climate simulations have to be downscaled. The statistical nature of SCAMP also allows to account for the uncertainty in the downscaling relationship. The ensemble of weather scenarios generated by SCAMP for any large-scale scenario allows thus to simulate and account for the small-scale internal variability of weather. This is another advantage over MAR, allowing a more robust assessment of possible low-frequency changes in hydro-meteorological regimes (e.g. Lafaysse et al., 2014; Raynaud et al., 2020). In a future study, we will force the SCAMP/GSM-SOCONT chain with a CMIP6-PMIP4 paleosimulation ensemble (Jungclaus et al., 2017; Kageyama et al., 2018) to assess the variations of hydro-meteorological regimes of the URR catchment over the last millenium. We also expect to confront the simulated variations in flood activity with those obtained in previous works from the sediments archives of Lake Bourget (Jenny et al., 2014; Wilhelm et al., 2022). Moreover, this could also corroborate the influence of warming and atmospheric circulation changes on multi-decadal flood activity over the last two centuries, recently highlighted by Brönnimann et al. (2022) for different European rivers.

As already shown in previous works, the hydrological behavior of river basins can be simulated from large-scale atmospheric information only. In the present work, we also show that the simulation of relevant hydrological scenarios requires a BC of the downscaled weather scenarios. The highly non-linear behavior of hydrological systems does actually not bear biased weather. This was made evident here for temperature, due to the highly non-linear thermal sensitivity of snow variables. If it seeks to be relevant, BC is not necessarily simple (Switanek et al., 2022; Robin et al., 2023). For temperature, BC is typically applied for the temperature of reference stations. For the URR catchment, it was also needed for the temperature lapse rate simulated by the dynamical downscaling model MAR. The temperature lapse rate correction was determinant to avoid irrelevant simulations of the snowpack dynamics at high elevations, and consequently of the hydrology.

BC is also required for precipitation. Significant differences were also found between reference and downscaled precipitation, particularly for MAR in winter. BC of downscaled precipitation was thus also applied so that the statistical distribution of precipitation scenarios fits that of reference. But the quality of the reference is questionable. It was indeed developed disregarding the significant precipitation-elevation relationship in the area, to avoid the simulation of irrelevant flood events. The much larger precipitation amounts simulated by MAR for high elevation sub-basins are thus not necessarily irrelevant, despite the snowfall undercatch issues (Kochendorfer et al., 2017). A better understanding of the precipitation-elevation relationship in mountainous areas, especially its likely variations in time and dependence on event types, would improve hydro-meteorological analyses and simulations and make them more relevant. This would benefit from more observations in high altitude areas, a critical issue pointed out for a long time (e.g. Hingray et al., 2012). Despite their multiple limitations in mountainous areas, radar data could also provide valuable insights into orographic drivers of precipitation (e.g. Germann et al., 2022).

https://doi.org/10.5194/hess-2023-92
Preprint. Discussion started: 20 April 2023


If downscaling models clearly need to be refined in the future, scientists should also consider improving BC methods for such challenging configurations. They should also consider the possibility of better understanding and accounting for event-scale precipitation orographic enhancement in the models. Dynamical downscaling models such as MAR are likely promising tools for such analyses, but their value for areas with marked relief should be better estimated.

*Author contributions.* This study is part of CL's PhD thesis. BW and BH supervised the PhD. All authors contributed to the design of the study and the analysis framework. CL performed the simulations and produced the figures presented in this study. CL, MM and BH contributed to the writing of the document and to the editing of the paper.

*Competing interests.* The authors declare that they have no conflict of interest.

*Acknowledgements.* This work was supported by the French National Research Agency in the framework of the "Investissements d'avenir" program (ANR-15-IDEX-02). A part of the simulations could be performed from the Grenoble Alpes Research Data and Computing Infrastructure GRICAD (https://gricad.univ-grenoble-alpes.fr/, last access: 20 February 2023). We would especially like to thank Mondher Chekki for its precious technical and informatic help, and Julien Beaumet for providing the outputs of the MAR simulation.

https://doi.org/10.5194/hess-2023-92
Preprint. Discussion started: 20 April 2023


Hydrology and Earth System Sciences
Discussions

## References

Arnell, N. W., Hudson, D. A., and Jones, R. G.: Climate change scenarios from a regional climate model: Estimating change in runoff in southern Africa, J. Geophys. Res., 108, 4519, https://doi.org/10.1029/2002JD002782, 2003.

Beaumet, J., Ménégoz, M., Morin, S., Gallée, H., Fettweis, X., Six, D., Vincent, C., Wilhelm, B., and Anquetin, S.: Twentieth century temperature and snow cover changes in the French Alps, Reg. Environ. Change, 21, 114, https://doi.org/10.1007/s10113-021-01830-x, 2021.

Bechtold, P., Bazile, E., Guichard, F., Mascart, P., and Richard, E.: A mass-flux convection scheme for regional and global models, Q. J. Roy. Meteorol. Soc., 127, 869–886, https://doi.org/10.1002/qj.49712757309, 2001.

Ben Daoud, A., Sauquet, E., Bontron, G., Obled, C., and Lang, M.: Daily quantitative precipitation forecasts based on the analogue method: Improvements and application to a French large river basin, Atmos. Res., 169, 147–159, https://doi.org/10.1016/j.atmosres.2015.09.015, 2016.

Beniston, M.: Mountain Weather and Climate: A General Overview and a Focus on Climatic Change in the Alps, Hydrobiologia, 562, 3–16, https://doi.org/10.1007/s10750-005-1802-0, 2006.

Blöschl, G., Hall, J., Parajka, J., Perdigão, R. A. P., Merz, B., Arheimer, B., Aronica, G. T., Bilibashi, A., Bonacci, O., Borga, M., Čanjevac, I., Castellarin, A., Chirico, G. B., Claps, P., Fiala, K., Frolova, N., Gorbachova, L., Gül, A., Hannaford, J., Harrigan, S., Kireeva, M., Kiss, A., Kjeldsen, T. R., Kohnová, S., Koskela, J. J., Ledvinka, O., Macdonald, N., Mavrova-Guirguinova, M., Mediero, L., Merz, R., Molnar, P., Montanari, A., Murphy, C., Osuch, M., Ovcharuk, V., Radevski, I., Rogger, M., Salinas, J. L., Sauquet, E., Šraj, M., Szolgay, J., Viglione, A., Volpi, E., Wilson, D., Zaimi, K., and Živković, N.: Changing climate shifts timing of European floods, Science, 357, 588–590, https://doi.org/10.1126/science.aan2506, 2017.

Boé, J., Terray, L., Habets, F., and Martin, E.: Statistical and dynamical downscaling of the Seine basin climate for hydro-meteorological studies, Int. J. Climatol., 27, 1643–1655, https://doi.org/10.1002/joc.1602, 2007.

Brun, E., David, P., Sudul, M., and Brunot, G.: A numerical model to simulate snow-cover stratigraphy for operational avalanche forecasting, J. Glaciol., 38, 13–22, https://doi.org/10.3189/S0022143000009552, 1992.

Brönnimann, S., Stucki, P., Franke, J., Valler, V., Brugnara, Y., Hand, R., Slivinski, L. C., Compo, G. P., Sardeshmukh, P. D., Lang, M., and Schaefli, B.: Influence of warming and atmospheric circulation changes on multidecadal European flood variability, Clim. Past, 18, 919–933, https://doi.org/10.5194/cp-18-919-2022, 2022.

Bárdossy, A.: Calibration of hydrological model parameters for ungauged catchments, Hydrol. Earth Syst. Sci., 11, 703–710, https://doi.org/10.5194/hess-11-703-2007, 2007.

Bárdossy, A. and Pegram, G.: Interpolation of precipitation under topographic influence at different time scales: Interpolation of Precipitation, Water Resour. Res., 49, 4545–4565, https://doi.org/10.1002/wrcr.20307, 2013.

Caillouet, L., Vidal, J.-P., Sauquet, E., and Graff, B.: Probabilistic precipitation and temperature downscaling of the Twentieth Century Reanalysis over France, Clim. Past, 12, 635–662, https://doi.org/10.5194/cp-12-635-2016, 2016.

Caillouet, L., Vidal, J.-P., Sauquet, E., Devers, A., and Graff, B.: Ensemble reconstruction of spatio-temporal extreme low-flow events in France since 1871, Hydrol. Earth Syst. Sci., 21, 2923–2951, https://doi.org/10.5194/hess-21-2923-2017, 2017.

CERCG: Règlement sur la manoeuvre de l'ouvrage de régularisation du niveau du lac Léman à Genève. Arrêté du 17 septembre 1997, Genève, Suisse, 1997.

https://doi.org/10.5194/hess-2023-92
Preprint. Discussion started: 20 April 2023




Chagnaud, G., Gallée, H., Lebel, T., Panthou, G., and Vischel, T.: A Boundary Forcing Sensitivity Analysis of the West African Monsoon Simulated by the Modèle Atmosphérique Régional, Atmosphere, 11, 191, https://doi.org/10.3390/atmos11020191, 2020.

Chardon, J., Hingray, B., Favre, A.-C., Autin, P., Gailhard, J., Zin, I., and Obled, C.: Spatial Similarity and Transferability of Analog Dates for Precipitation Downscaling over France, J. Climate, 27, 5056–5074, https://doi.org/10.1175/JCLI-D-13-00464.1, 2014.

Chardon, J., Favre, A.-C., and Hingray, B.: Effects of Spatial Aggregation on the Accuracy of Statistically Downscaled Precipitation Predictions, J. Hydrometeorol., 17, 1561–1578, https://doi.org/10.1175/JHM-D-15-0031.1, 2016.

Chardon, J., Hingray, B., and Favre, A.-C.: An adaptive two-stage analog/regression model for probabilistic prediction of small-scale precipitation in France, Hydrol. Earth Syst. Sci., 22, 265–286, https://doi.org/10.5194/hess-22-265-2018, 2018.

Clark, M., Gangopadhyay, S., Hay, L., Rajagopalan, B., and Wilby, R.: The Schaake Shuffle: A Method for Reconstructing Space-Time Variability in Forecasted Precipitation and Temperature Fields, J. Hydrometeorol., 5, 243–262, https://doi.org/10.1175/1525-7541(2004)005<0243:TSSAMF>2.0.CO;2, 2004.

Dayon, G., Boe, J., and Martin, E.: Transferability in the future climate of a statistical downscaling method for precipitation in France, J. Geophys. Res.-Atmos., 120, 1023–1043, https://doi.org/10.1002/2014JD022236, 2015.

De Ridder, K. and Schayes, G.: The IAGL Land Surface Model, J. Appl. Meteorol., 36, 167–182, https://doi.org/10.1175/1520-0450(1997)036<0167:TILSM>2.0.CO;2, 1997.

Di Sante, F., Coppola, E., and Giorgi, F.: Projections of river floods in Europe using EURO-CORDEX, CMIP5 and CMIP6 simulations, Int. J. Climatol., 41, 3203–3221, https://doi.org/10.1002/joc.7014, 2021.

Doutreloup, S., Wyard, C., Amory, C., Kittel, C., Erpicum, M., and Fettweis, X.: Sensitivity to Convective Schemes on Precipitation Simulated by the Regional Climate Model MAR over Belgium (1987–2017), Atmosphere, 10, 34, https://doi.org/10.3390/atmos10010034, 2019.

Déqué, M.: Frequency of precipitation and temperature extremes over France in an anthropogenic scenario: Model results and statistical correction according to observed values, Global Planet. Change, 57, 16–26, https://doi.org/10.1016/j.gloplacha.2006.11.030, 2007.

Evin, G., Somot, S., and Hingray, B.: Balanced estimate and uncertainty assessment of European climate change using the large EURO-CORDEX regional climate model ensemble, Earth Syst. Dynam., 12, 1543–1569, https://doi.org/10.5194/esd-12-1543-2021, 2021.

Fowler, H. J., Blenkinsop, S., and Tebaldi, C.: Linking climate change modelling to impacts studies: recent advances in downscaling techniques for hydrological modelling, Int. J. Climatol., 27, 1547–1578, https://doi.org/10.1002/joc.1556, 2007.

Froidurot, S., Zin, I., Hingray, B., and Gautheron, A.: Sensitivity of Precipitation Phase over the Swiss Alps to Different Meteorological Variables, J. Hydrometeorol., 15, 685–696, https://doi.org/10.1175/JHM-D-13-073.1, 2014.

Gallée, H.: Simulation of the Mesocyclonic Activity in the Ross Sea, Antarctica, Mon. Weather Rev., 123, 2051–2069, https://doi.org/10.1175/1520-0493(1995)123<2051:SOTMAI>2.0.CO;2, 1995.

Gallée, H. and Duynkerke, P. G.: Air-snow interactions and the surface energy and mass balance over the melting zone of west Greenland during the Greenland Ice Margin Experiment, J. Geophys. Res.-Atmos., 102, 13 813–13 824, https://doi.org/10.1029/96JD03358, 1997.

Gallée, H. and Schayes, G.: Development of a 3-Dimensional Meso-Gamma Primitive Equation Model - Katabatic Winds Simulation in the Area of Terra-Nova Bay, Antarctica, Mon. Weather Rev., 122, 671–685, https://doi.org/10.1175/1520-0493(1994)122<0671:DOATDM>2.0.CO;2, 1994.

Gallée, H., Pettré, P., and Schayes, G.: Sudden Cessation of Katabatic Winds in Adélie Land, Antarctica, J. Appl. Meteorol., 35, 1142–1152, https://doi.org/10.1175/1520-0450(1996)035<1142:SCOKWI>2.0.CO;2, 1996.

https://doi.org/10.5194/hess-2023-92
Preprint. Discussion started: 20 April 2023




Gallée, H., Guyomarc'h, G., and Brun, E.: Impact Of Snow Drift On The Antarctic Ice Sheet Surface Mass Balance: Possible Sensitivity To Snow-Surface Properties, Bound.-Lay. Meteorol., 99, 1–19, https://doi.org/10.1023/A:1018776422809, 2001.

Gangopadhyay, S., Clark, M., and Rajagopalan, B.: Statistical downscaling using K-nearest neighbors, Water Resour. Res., 41, W02 024, https://doi.org/10.1029/2004WR003444, 2005.

Germann, U., Boscacci, M., Clementi, L., Gabella, M., Hering, A., Sartori, M., Sideris, I. V., and Calpini, B.: Weather Radar in Complex Orography, Remote Sens., 14, 503, https://doi.org/10.3390/rs14030503, 2022.

Giorgi, F. and Mearns, L. O.: Approaches to the simulation of regional climate change: A review, Rev. Geophys., 29, 191–216, https://doi.org/10.1029/90RG02636, 1991.

GLIMS: Glacier Database. Boulder Colorado, USA. NASA National Snow and Ice Data Center Distributed Active Archive Center, https://doi.org/10.7265/N5V98602, last access: 12 September 2020, 2019.

Grandjean, P.: La régularisation du lac Léman, 1990.

Hanssen-Bauer, I., Achberger, C., Benestad, R. E., Chen, D., and Førland, E. J.: Statistical downscaling of climate scenarios over Scandinavia, Climate Res., 29, 255–268, https://doi.org/10.3354/cr029255, 2005.

Harris, I., Jones, P., Osborn, T., and Lister, D.: Updated high-resolution grids of monthly climatic observations - the CRU TS3.10 Dataset, Int. J. Climatol., 34, 623–642, https://doi.org/10.1002/joc.3711, 2014.

Hay, L. E., Clark, M. P., Wilby, R. L., Gutowski, W. J., Leavesley, G. H., Pan, Z., Arritt, R. W., and Takle, E. S.: Use of Regional Climate Model Output for Hydrologic Simulations, J. Hydrometeorol., 3, 571–590, https://doi.org/10.1175/1525-7541(2002)003<0571:UORCMO>2.0.CO;2, 2002.

Hersbach, H., Bell, B., Berrisford, P., Hirahara, S., Horányi, A., Muñoz-Sabater, J., Nicolas, J., Peubey, C., Radu, R., Schepers, D., Simmons, A., Soci, C., Abdalla, S., Abellan, X., Balsamo, G., Bechtold, P., Biavati, G., Bidlot, J., Bonavita, M., Chiara, G., Dahlgren, P., Dee, D., Diamantakis, M., Dragani, R., Flemming, J., Forbes, R., Fuentes, M., Geer, A., Haimberger, L., Healy, S., Hogan, R. J., Hólm, E., Janisková, M., Keeley, S., Laloyaux, P., Lopez, P., Lupu, C., Radnoti, G., Rosnay, P., Rozum, I., Vamborg, F., Villaume, S., and Thépaut, J.: The ERA5 global reanalysis, Q. J. Roy. Meteorol. Soc., 146, 1999–2049, https://doi.org/10.1002/qj.3803, 2020.

Hingray, B., Schaefli, B., Mezghani, A., and Hamdi, Y.: Signature-based model calibration for hydrological prediction in mesoscale Alpine catchments, Hydrolog. Sci. J., 55, 1002–1016, https://doi.org/10.1080/02626667.2010.505572, 2010.

Hingray, B., Dedieu, J.-P., Lebel, T., Obled, C., Sicart, J.-E., Six, D., Vincent, C., Wagnon, P., and Zin, I.: Observations glaciologiques et hydrométéorologiques en zone de montagne : quelques problématiques et perspectives actuelles, La Houille Blanche, 2, 5–11, https://doi.org/10.1051/lhb/2012009, 2012.

Hingray, B., Picouet, C., and Musy, A.: Hydrology A Science for Engineers, CRC Press, 592 pp., ISBN 9781466590595, 2014.

Horton, P. and Brönnimann, S.: Impact of global atmospheric reanalyses on statistical precipitation downscaling, Clim. Dynam., 52, 5189–5211, https://doi.org/10.1007/s00382-018-4442-6, 2019.

Isotta, F. A., Frei, C., Weilguni, V., Tadic, M. P., Lassegues, P., Rudolf, B., Pavan, V., Cacciamani, C., Antolini, G., Ratto, S. M., Munari, M., Micheletti, S., Bonati, V., Lussana, C., Ronchi, C., Panettieri, E., Marigo, G., and Vertacnik, G.: The climate of daily precipitation in the Alps: development and analysis of a high-resolution grid dataset from pan-Alpine rain-gauge data, Int. J. Climatol., 34, 1657–1675, https://doi.org/10.1002/joc.3794, 2014.

Jenny, J.-P., Wilhelm, B., Arnaud, F., Sabatier, P., Giguet Covex, C., Mélo, A., Fanget, B., Malet, E., Ployon, E., and Perga, M. E.: A 4D sedimentological approach to reconstructing the flood frequency and intensity of the Rhône River (Lake Bourget, NW European Alps), J. Paleolimnol., 51, 469–483, https://doi.org/10.1007/s10933-014-9768-4, 2014.



Jha, M., Pan, Z. T., Takle, E. S., and Gu, R.: Impacts of climate change on streamflow in the Upper Mississippi River Basin: A regional climate model perspective, J. Geophys. Res., 109, D09 105, https://doi.org/10.1029/2003JD003686, 2004.

Jungclaus, J. H., Bard, E., Baroni, M., Braconnot, P., Cao, J., Chini, L. P., Egorova, T., Evans, M., González-Rouco, J. F., Goosse, H., Hurtt, G. C., Joos, F., Kaplan, J. O., Khodri, M., Klein Goldewijk, K., Krivova, N., LeGrande, A. N., Lorenz, S. J., Luterbacher, J., Man, W., Maycock, A. C., Meinshausen, M., Moberg, A., Muscheler, R., Nehrbass-Ahles, C., Otto-Bliesner, B. I., Phipps, S. J., Pongratz, J., Rozanov, E., Schmidt, G. A., Schmidt, H., Schmutz, W., Schurer, A., Shapiro, A. I., Sigl, M., Smerdon, J. E., Solanki, S. K., Timmreck, C., Toohey, M., Usoskin, I. G., Wagner, S., Wu, C.-J., Yeo, K. L., Zanchettin, D., Zhang, Q., and Zorita, E.: The PMIP4 contribution to CMIP6 - Part 3: The last millennium, scientific objective, and experimental design for the PMIP4 past1000 simulations, Geosci. Model Dev., 10, 4005–4033, https://doi.org/10.5194/gmd-10-4005-2017, 2017.

Kageyama, M., Braconnot, P., Harrison, S. P., Haywood, A. M., Jungclaus, J. H., Otto-Bliesner, B. L., Peterschmitt, J.-Y., Abe-Ouchi, A., Albani, S., Bartlein, P. J., Brierley, C., Crucifix, M., Dolan, A., Fernandez-Donado, L., Fischer, H., Hopcroft, P. O., Ivanovic, R. F., Lambert, F., Lunt, D. J., Mahowald, N. M., Peltier, W. R., Phipps, S. J., Roche, D. M., Schmidt, G. A., Tarasov, L., Valdes, P. J., Zhang, Q., and Zhou, T.: The PMIP4 contribution to CMIP6 - Part 1: Overview and over-arching analysis plan, Geosci. Model Dev., 11, 1033–1057, https://doi.org/10.5194/gmd-11-1033-2018, 2018.

Kochendorfer, J., Rasmussen, R., Wolff, M., Baker, B., Hall, M. E., Meyers, T., Landolt, S., Jachcik, A., Isaksen, K., Brækkan, R., and Leeper, R.: The quantification and correction of wind-induced precipitation measurement errors, Hydrol. Earth Syst. Sci., 21, 1973–1989, https://doi.org/10.5194/hess-21-1973-2017, 2017.

Kuchment, L. and Gelfan, A.: The determination of the snowmelt rate and the meltwater outflow from a snowpack for modelling river runoff generation, J. Hydrol., 179, 23–36, https://doi.org/10.1016/0022-1694(95)02878-1, 1996.

Kuentz, A., Mathevet, T., Gailhard, J., and Hingray, B.: Building long-term and high spatio-temporal resolution precipitation and air temperature reanalyses by mixing local observations and global atmospheric reanalyses: the ANATEM model, Hydrol. Earth Syst. Sci., 19, 2717–2736, https://doi.org/10.5194/hess-19-2717-2015, 2015.

Kundzewicz, Z. W., Krysanova, V., Dankers, R., Hirabayashi, Y., Kanae, S., Hattermann, F. F., Huang, S., Milly, P. C. D., Stoffel, M., Driessen, P. P. J., Matczak, P., Quevauviller, P., and Schellnhuber, H.-J.: Differences in flood hazard projections in Europe - their causes and consequences for decision making, Hydrolog. Sci. J., 62, 1–14, https://doi.org/10.1080/02626667.2016.1241398, 2016.

Lafaysse, M., Hingray, B., Mezghani, A., Gailhard, J., and Terray, L.: Internal variability and model uncertainty components in future hydrometeorological projections: The Alpine Durance basin, Water Resour. Res., 50, 3317–3341, https://doi.org/10.1002/2013WR014897, 2014.

Leander, R., Buishand, T. A., van den Hurk, B. J. J. M., and de Wit, M. J. M.: Estimated changes in flood quantiles of the river Meuse from resampling of regional climate model output, J. Hydrol., 351, 331–343, https://doi.org/10.1016/j.jhydrol.2007.12.020, 2008.

Lemaitre-Basset, T., Collet, L., Thirel, G., Parajka, J., Evin, G., and Hingray, B.: Climate change impact and uncertainty analysis on hydrological extremes in a French Mediterranean catchment, Hydrolog. Sci. J., 66, 888–903, https://doi.org/10.1080/02626667.2021.1895437, 2021.

Leung, L. R. and Qian, Y.: Atmospheric rivers induced heavy precipitation and flooding in the western US simulated by the WRF regional climate model, Geophys. Res. Lett., 36, L03 820, https://doi.org/10.1029/2008GL036445, 2009.

Lorenz, E. N.: Atmospheric Predictability as Revealed by Naturally Occurring Analogues, J. Atmos. Sci., 26, 636–646, https://doi.org/10.1175/1520-0469(1969)26<636:APARBN>2.0.CO;2, 1969.

https://doi.org/10.5194/hess-2023-92
Preprint. Discussion started: 20 April 2023




Maraun, D., Wetterhall, F., Ireson, A. M., Chandler, R. E., Kendon, E. J., Widmann, M., Brienen, S., Rust, H. W., Sauter, T., Themeßl, M., Venema, V. K. C., Chun, K. P., Goodess, C. M., Jones, R. G., Onof, C., Vrac, M., and Thiele-Eich, I.: Precipitation downscaling under climate change: Recent developments to bridge the gap between dynamical models and the end user, Rev. Geophys., 48, RG3003, https://doi.org/10.1029/2009RG000314, 2010.

Marty, R., Zin, I., Obled, C., Bontron, G., and Djerboua, A.: Toward Real-Time Daily PQPF by an Analog Sorting Approach: Application to Flash-Flood Catchments, J. Appl. Meteorol. Clim., 51, 505–520, https://doi.org/10.1175/JAMC-D-11-011.1, 2012.

Masson-Delmotte, V., Zhai, P., Pirani, A., Connors, S. L., Péan, C., Berger, S., Caud, N., Chen, Y., Goldfarb, L., Gomis, M. I., Huang, M., Leitzell, K., Lonnoy, E., Matthews, J. B. R., Maycock, T. K., Waterfield, T., Yelekçi, O., Yu, R., and Zhou, B.: Climate Change 2021: The Physical Science Basis. Contribution of Working Group I to the Sixth Assessment Report of the Intergovernmental Panel on Climate Change, Cambridge University Press, Cambridge, United Kingdom and New York, NY, USA, 2391 pp., https://doi.org/978-1-00-915789-6, 2021.

Mezghani, A. and Hingray, B.: A combined downscaling-disaggregation weather generator for stochastic generation of multisite hourly weather variables over complex terrain: Development and multi-scale validation for the Upper Rhone River basin, J. Hydrol., 377, 245–260, https://doi.org/10.1016/j.jhydrol.2009.08.033, 2009.

Ménégoz, M., Gallée, H., and Jacobi, H. W.: Precipitation and snow cover in the Himalaya: from reanalysis to regional climate simulations, Hydrol. Earth Syst. Sci., 17, 3921–3936, https://doi.org/10.5194/hess-17-3921-2013, 2013.

Ménégoz, M., Valla, E., Jourdain, N. C., Blanchet, J., Beaumet, J., Wilhelm, B., Gallée, H., Fettweis, X., Morin, S., and Anquetin, S.: Contrasting seasonal changes in total and intense precipitation in the European Alps from 1903 to 2010, Hydrol. Earth Syst. Sci., 24, 5355–5377, https://doi.org/10.5194/hess-24-5355-2020, 2020.

Nash, J. and Sutcliffe, J.: River flow forecasting through conceptual models part I - A discussion of principles, J. Hydrol., 10, 282–290, https://doi.org/10.1016/0022-1694(70)90255-6, 1970.

Obled, C., Bontron, G., and Garçon, R.: Quantitative precipitation forecasts: a statistical adaptation of model outputs through an analogues sorting approach, Atmos. Res., 63, 303–324, https://doi.org/10.1016/S0169-8095(02)00038-8, 2002.

Obled, C., Zin, I., and Hingray, B.: Choix des pas de temps et d'espace pour des modélisations parcimonieuses en hydrologie des crues, La Houille Blanche, 5, 81–87, https://doi.org/10.1051/lhb/2009059, 2009.

Poli, P., Hersbach, H., Dee, D. P., Berrisford, P., Simmons, A. J., Vitart, F., Laloyaux, P., Tan, D. G. H., Peubey, C., Thépaut, J.-N., Trémolet, Y., Hólm, E. V., Bonavita, M., Isaksen, L., and Fisher, M.: ERA-20C: An Atmospheric Reanalysis of the Twentieth Century, J. Climate, 29, 4083–4097, https://doi.org/10.1175/JCLI-D-15-0556.1, 2016.

Raymond, F., Wilhelm, B., and Anquetin, S.: Is Precipitation the Main Trigger of Medium-Magnitude Floods in Large Alpine Catchments?, Water, 11, 2507, https://doi.org/10.3390/w11122507, 2019.

Raynaud, D., Hingray, B., Evin, G., Favre, A.-C., and Chardon, J.: Assessment of meteorological extremes using a synoptic weather generator and a downscaling model based on analogues, Hydrol. Earth Syst. Sci., 24, 4339–4352, https://doi.org/10.5194/hess-24-4339-2020, 2020.

Robin, Y., Corre, L., Marson, P., Bernus, M., Vrac, M., and Thao, S.: Projections climatiques régionalisées pour la France : corrections de biais et changements futurs. Rapport Climat du projet Explore2 : des futurs de l'eau. Inrae, Météo France, IPSL. Financement : Office Fédéral de la Biodiversité, Ministère de la Transition Ecologique, https://professionnels.ofb.fr/fr/node/1244, last access: 20 February 2023, 2023.

Rohwer, C.: Evaporation from free water surfaces, Technical Bulletin No. 271, United States, Department of Agriculture, https://doi.org/DOI: 10.22004/ag.econ.163103, 1931.

https://doi.org/10.5194/hess-2023-92
Preprint. Discussion started: 20 April 2023


Hydrology and Earth System Sciences
Discussions

Roudier, P., Andersson, J. C. M., Donnelly, C., Feyen, L., Greuell, W., and Ludwig, F.: Projections of future floods and hydrological droughts in Europe under a +2°C global warming, Clim. Change, 135, 341–355, https://doi.org/10.1007/s10584-015-1570-4, 2016.

Ruelland, D.: Should altitudinal gradients of temperature and precipitation inputs be inferred from key parameters in snow-hydrological models?, Hydrol. Earth Syst. Sci., 24, 2609–2632, https://doi.org/10.5194/hess-24-2609-2020, 2020.

Ruosteenoja, K., Markkanen, T., Venäläinen, A., Räisänen, P., and Peltola, H.: Seasonal soil moisture and drought occurrence in Europe in CMIP5 projections for the 21st century, Clim. Dynam., 50, 1177–1192, https://doi.org/10.1007/s00382-017-3671-4, 2018.

Salathé, E. P., Hamlet, A. F., Mass, C. F., Lee, S.-Y., Stumbaugh, M., and Steed, R.: Estimates of Twenty-First-Century Flood Risk in the Pacific Northwest Based on Regional Climate Model Simulations, J. Hydrometeorol., 15, 1881–1899, https://doi.org/10.1175/JHM-D-13-0137.1, 2014.

Schaefli, B., Hingray, B., Niggli, M., and Musy, A.: A conceptual glacio-hydrological model for high mountainous catchments, Hydrol. Earth Syst. Sci., 9, 95–109, https://doi.org/10.5194/hess-9-95-2005, 2005.

Sivapalan, M., Blöschl, G., Zhang, L., and Vertessy, R.: Downward approach to hydrological prediction, Hydrol. Process., 17, 2101–2111, https://doi.org/10.1002/hyp.1425, 2003.

Switanek, M., Maraun, D., and Bevacqua, E.: Stochastic downscaling of gridded precipitation to spatially coherent subgrid precipitation fields using a transformed Gaussian model, Int. J. Climatol., 42, 6126–6147, https://doi.org/10.1002/joc.7581, 2022.

Tapiador, F. J., Navarro, A., Moreno, R., Sánchez, J. L., and García-Ortega, E.: Regional climate models: 30 years of dynamical downscaling, Atmos. Res., 235, 104 785, https://doi.org/10.1016/j.atmosres.2019.104785, 2020.

Teweles, S. and Wobus, H. B.: Verification of Prognostic Charts, B. Am. Meteorol. Soc., 35, 455–463, https://doi.org/10.1175/1520-0477-35.10.455, 1954.

Tolson, B. A. and Shoemaker, C. A.: Dynamically dimensioned search algorithm for computationally efficient watershed model calibration, Water Resour. Res., 43, W01 413, https://doi.org/10.1029/2005WR004723, 2007.

Vidal, J.-P., Hingray, B., Magand, C., Sauquet, E., and Ducharne, A.: Hierarchy of climate and hydrological uncertainties in transient low-flow projections, Hydrol. Earth Syst. Sci., 20, 3651–3672, https://doi.org/10.5194/hess-20-3651-2016, 2016.

Viviroli, D., Mittelbach, H., Gurtz, J., and Weingartner, R.: Continuous simulation for flood estimation in ungauged mesoscale catchments of Switzerland - Part II: Parameter regionalisation and flood estimation results, J. Hydrol., 377, 208–225, https://doi.org/10.1016/j.jhydrol.2009.08.022, 2009.

Viviroli, D., Sikorska-Senoner, A. E., Evin, G., Staudinger, M., Kauzlaric, M., Chardon, J., Favre, A.-C., Hingray, B., Nicolet, G., Raynaud, D., Seibert, J., Weingartner, R., and Whealton, C.: Comprehensive space–time hydrometeorological simulations for estimating very rare floods at multiple sites in a large river basin, Nat. Hazards Earth Syst. Sci., 22, 2891–2920, https://doi.org/10.5194/nhess-22-2891-2022, 2022.

Von Storch, H., Zorita, E., and Cubasch, U.: Downscaling of Global Climate-Change Estimates to Regional Scales - an Application to Iberian Rainfall in Wintertime, J. Climate, 6, 1161–1171, https://doi.org/10.1175/1520-0442(1993)006<1161:DOGCCE>2.0.CO;2, 1993.

Wilby, R., Hay, L., and Leavesley, G.: A comparison of downscaled and raw GCM output: implications for climate change scenarios in the San Juan River basin, Colorado, J. Hydrol., 225, 67–91, https://doi.org/10.1016/S0022-1694(99)00136-5, 1999.

Wilby, R. L. and Quinn, N. W.: Reconstructing multi-decadal variations in fluvial flood risk using atmospheric circulation patterns, J. Hydrol., 487, 109–121, https://doi.org/10.1016/j.jhydrol.2013.02.038, 2013.

https://doi.org/10.5194/hess-2023-92
Preprint. Discussion started: 20 April 2023




Wilhelm, B., Rapuc, W., Amann, B., Anselmetti, F. S., Arnaud, F., Blanchet, J., Brauer, A., Czymzik, M., Giguet-Covex, C., Gilli, A., Glur, L., Grosjean, M., Irmler, R., Nicolle, M., Sabatier, P., Swierczynski, T., and Wirth, S. B.: Impact of warmer climate periods on flood hazard in the European Alps, Nat. Geosci., 15, 118–123, https://doi.org/10.1038/s41561-021-00878-y, 2022.

Winsemius, H. C., Schaefli, B., Montanari, A., and Savenije, H. H. G.: On the calibration of hydrological models in ungauged basins: A framework for integrating hard and soft hydrological information, Water Resour. Res., 45, W12 422, https://doi.org/10.1029/2009WR007706, 2009.

Wyard, C., Scholzen, C., Fettweis, X., Van Campenhout, J., and François, L.: Decrease in climatic conditions favouring floods in the southeast of Belgium over 1959-2010 using the regional climate model MAR, Int. J. Climatol., 37, 2782–2796, https://doi.org/10.1002/joc.4879, 2017.